



universität  
wien

# DIPLOMARBEIT

Titel der Diplomarbeit

## Application of Ionic Liquid Matrices in MALDI-Mass Spectrometry of Peptides, Glycopeptides and Glycans

Verfasserin

Manuela Kropik

angestrebter akademischer Grad

Magistra der Naturwissenschaften (Mag. rer. nat.)

Wien, 2010

Studienkennzahl lt. Studienblatt:

A 419

Studienrichtung lt. Studienblatt:

Chemie

Betreuerin / Betreuer:

Univ.-Prof. Dr. Andreas Rizzi



## DANKSAGUNG

An dieser Stelle möchte ich mich bei allen bedanken, die mir die Diplomarbeit ermöglicht bzw. mich in dieser Zeit begleitet haben.

Ganz speziell bedanken möchte ich mich bei Herrn Prof. Rizzi für die interessante Aufgabenstellung und seine ausgezeichnete Betreuung.

Bei meinen Kollegen Dr. Michael Lechner möchte ich mich für seine Unterstützung und das angenehme Arbeitsklima bedanken.

Bei meiner ganzen Familie, besonders bei meiner Schwester Tina und bei Philipp, und auch bei meinen Freunden Petra, Jasmin und Franz möchte ich mich bedanken, für alle aufbauenden Worte und guten Ratschläge, die mir auf dem Weg zum Abschluss dieses Studiums sehr geholfen haben.



# Table of content

List of abbreviations .....	7
<b>1. Introduction.....</b>	<b>9</b>
1.1. Aim of the work .....	11
1.2. Ionic liquids .....	12
1.2.1. Characteristics of ionic liquids .....	12
1.2.2. Applications of ILs in analytical chemistry .....	12
1.3. ILs as matrices for MALDI-MS .....	14
1.3.1. The role of the matrix in the MALDI process .....	14
1.3.2. The introduction of ILs as MALDI matrices .....	15
1.3.3. Sample homogeneity in ionic liquid matrices .....	16
1.3.4. Substances which can be analyzed in ILMs .....	16
1.3.5. Sensitivity and adduct formation in ILMs .....	17
1.3.6. Fragmentation of analytes .....	18
1.3.7. Quantitative analysis .....	19
1.3.8. MALDI imaging .....	20
<b>2. Experimental .....</b>	<b>21</b>
2.1. Materials .....	21
2.2. Sample preparation.....	21
2.3. Preparation of the ionic liquids .....	22
2.4. Matrix solutions and sample preparation for MALDI-MS analysis .....	22
2.5. Mass spectrometry.....	24
<b>3. Results and Discussion .....</b>	<b>26</b>
3.1. Ionic liquid matrices.....	26
3.1.1. Properties of the investigated ionic liquids.....	26
3.1.2. ILM spot preparation: applied amount of ILM and film shape .....	27
3.2. Molecular Ions observed with ILMs.....	29
3.2.1. Molecular Ions formed in ILMs:.....	29
3.2.2. Effect of complexing additives on molecular ion formation .....	31
3.2.2.1. Di-ammonium hydrogen citrate as ILM solution additive.....	31

3.2.2.2. Di-ammonium hydrogen phosphate as ILM solution additive.....	32
<b>3.3. Ion suppression effects with ILMs .....</b>	<b>38</b>
3.3.1. Glycopeptides in peptide mixture.....	38
3.3.2. Cleaved glycans in peptide mixture .....	40
<b>3.4. Reduction of in-source and post-source decay by means of ILMs .....</b>	<b>44</b>
3.4.1. Sialylated glycopeptides in peptide mixture .....	44
3.4.2. Sialylated glycans in peptide mixture.....	45
<b>3.5. Enhancement of sensitivity and signal-to-noise ratio by means of ILMs .....</b>	<b>46</b>
3.5.1. Sensitivities of ILMs for peptides, glycopeptides and glycans in peptide mixture in comparison to the solid matrix THAP .....	46
3.5.2. Sequence coverage achieved using ILMs .....	47
<b>3.6. Modification in collision-induced dissociation pattern when using ILMs .....</b>	<b>51</b>
3.6.1. Glycopeptides.....	52
3.6.2. Glycans .....	54
<b>3.7. Reproducibility of quantitative pattern using ILMs .....</b>	<b>57</b>
<b>3.8. Conclusions .....</b>	<b>61</b>
 <b>4. Appendix .....</b>	 <b>64</b>
4.1. Chemical structure of ILM compounds.....	64
4.2. Ionic liquids used as matrices for MALDI-MS.....	65
4.3. Bovine $\alpha$ 1-acid-glycoprotein .....	66
4.3.1. The structure of bovine AGP .....	66
4.3.2. Glycosylation of bovine AGP .....	66
 <b>5. Literature .....</b>	 <b>67</b>
 <b>6. Abstract.....</b>	 <b>76</b>
 <b>7. Zusammenfassung.....</b>	 <b>78</b>
CURRICULUM VITAE.....	81

## **List of abbreviations**

<b>AC</b>	di-ammonium hydrogen citrate
<b>AGP</b>	$\alpha$ 1-acid-glycoprotein
<b>AP</b>	di-ammonium hydrogen phosphate
<b>BuA</b>	butylamine
<b>BuA-CHCA</b>	butylammonium $\alpha$ -cyano-4-hydroxycinnamate
<b>BuA-DHB</b>	butylammonium 2,5-dihydroxybenzoate
<b>BuA-THAP</b>	butylammonium 2,4,6-trihydroxyacetophenone
<b>CE</b>	capillary electrophoresis
<b>CHCA</b>	$\alpha$ -cyano-4-hydroxycinnamic acid
<b>CID</b>	collision-induced dissociation
<b>CIL</b>	chiral ionic liquid
<b>DHB</b>	2,5-dihydroxybenzoic acid
<b>DIEA</b>	<i>N,N</i> -diisopropylethylamine
<b>DIEA-CHCA</b>	<i>N,N</i> -diisopropylethylammonium $\alpha$ -cyano-4-hydroxycinnamate
<b>DIEA-DHB</b>	<i>N,N</i> -diisopropylethylammonium 2,5-dihydroxybenzoate
<b>DIEA-THAP</b>	<i>N,N</i> -diisopropylethylammonium 2,4,6-trihydroxyacetophenone
<b>DTT</b>	dithiothreitol
<b>ESI-MS</b>	electrospray ionization mass spectrometry
<b>GC</b>	gas chromatography
<b>GlcNAc</b>	<i>N</i> -acetyl-D-glucosamine
<b>Hex</b>	hexose
<b>HPLC</b>	high pressure liquid chromatography
<b>HxA</b>	hexylamine
<b>HxA-CHCA</b>	hexylammonium $\alpha$ -cyano-4-hydroxycinnamate
<b>HxA-DHB</b>	hexylammonium 2,5-dihydroxybenzoate
<b>HxA-THAP</b>	hexylammonium 2,4,6-trihydroxyacetophenone
<b>IL</b>	ionic liquid
<b>ILM</b>	ionic liquid matrix
<b>IR</b>	infrared

<b>ISD</b>	in-source decay
<b>LC</b>	liquid chromatography
<b>LOD</b>	limit of detection
<b><i>m/z</i></b>	mass-to-charge
<b>MALDI</b>	matrix-assisted laser desorption/ionisation
<b>MS</b>	mass spectrometry
<b>NeuNAc</b>	<i>N</i> -acetyl-neuraminic acid
<b>NeuNGI</b>	<i>N</i> -glycolyl-neuraminic acid
<b>NMR</b>	nuclear magnetic resonance
<b>PSD</b>	post-source decay
<b>PTM</b>	post-translational modification
<b>QIT</b>	quadrupole ion trap
<b>RSD</b>	relative standard deviations
<b>RTIL</b>	room-temperature ionic liquid
<b>rTOF</b>	reflector time-of-flight mass analyzer
<b>S/N</b>	signal-to-noise
<b>SA</b>	sialic acid
<b>TFA</b>	trifluoroacetic acid
<b>TGM</b>	<i>N,N,N',N'</i> -tetramethylguanidine
<b>TGM-CHCA</b>	<i>N,N,N',N'</i> -tetramethylguanidinium $\alpha$ -cyano-4-hydroxycinnamate
<b>TGM-DHB</b>	<i>N,N,N',N'</i> -tetramethylguanidinium 2,5-dihydroxybenzoate
<b>TGM-THAP</b>	<i>N,N,N',N'</i> -tetramethylguanidinium 2,4,6-trihydroxyacetophenone
<b>THAP</b>	2,4,6-trihydroxyacetophenone
<b>TRIS</b>	tris-(hydroxymethyl)-aminomethan hydrochloride
<b>UHQ</b>	water of ultra high quality
<b>UV</b>	ultraviolet



# **1. Introduction**

Protein glycosylation is one of the common post-translational modifications (PTMs) present in proteins of both eukaryotic [1] and prokaryotic [2] cells, and has a variety of structural and functional roles in membrane-associated and secreted proteins. Defining the structures and the attachment sites of the glycans present in glycoproteins is essential for understanding how glycosylation influences biological properties of proteins.

Mass spectrometry (MS) is a sensitive and powerful analytical technique for characterizing glycoproteins. There are two approaches for protein glycosylation analysis by MS: in the first one, the glycans are cleaved off from the amino acid backbone enzymatically or chemically and are analyzed as neat glycans, in the second one the glycoprotein is submitted to proteolysis yielding a mixture of peptides and glycopeptides which are analyzed by MS. This latter approach has the advantage providing site-specific information on glycosylation [3].

The analysis of protein glycosylation by glycopeptide-based MS is impaired by the ionization suppression of glycopeptides by the presence of non-glycosylated peptides. Glycopeptides consisting of a small peptide backbone and a rather large glycan structure exhibit low ionization efficiency. Therefore, the detection of small glycopeptides out of an unseparated enzymatic digest often fails. To overcome this problem and to detect glycopeptides present in proteolytic digests, pre-separation and/or derivatization of the analytes are usually applied.

As the matrix assisted laser desorption/ionization (MALDI) process produces mainly singly charged ions, easy interpretation of the mass spectra is possible and thus MALDI-MS finds particular use in the analysis of complex mixtures such as proteolytic digests. Furthermore, MALDI exhibits a moderate tolerance to salts and other contaminants.

In glycosylation research, however, the analysis of sialylated oligosaccharides might be problematic when using MALDI-MS because labile sialic acids are frequently dissociated during or shortly after the desorption/ionization process and thus ion species of intact molecules are hardly detected. Several methods for avoiding this loss have been reported, including stabilizing by derivatization of acidic parts [4],

permethylation of glycans [5], or use of “cool” matrixes, e.g., 2,4,6-trihydroxyacetophenone (THAP) [6]. A general weak point of MALDI-MS is the poor reproducibility of peak intensities because of inhomogeneous sample preparation. This might be overcome by the use of internal standards.

## **1.1. Aim of the work**

To acquire information regarding peptide sequence, glycosylation site and glycan composition of a glycopeptide by using MALDI-MS a careful selection of a well suited matrix and sample preparation technique is essential. The need for MS/MS analysis requires detection of glycopeptides with high intensity. Ionic liquid matrices (ILMs), introduced as an alternative to conventional crystalline matrices by Armstrong et al. [7], were reported not only to allow more homogeneous sample preparations but also to give favorable ionization yields for different types of analytes. Furthermore, ILMs are very “cool” matrices and thus less harsh conditions during the ionization/desorption process can be expected.

In this work, twelve different ionic liquids (ILs) were synthesized by combination of commonly used crystalline MALDI matrices, namely THAP,  $\alpha$ -Cyano-4-hydroxycinnamic acid (CHCA) and 2,5-dihydroxybenzoic acid (DHB), with four different organic bases. To avoid inhomogeneous analyte distribution, the focus was given on matrices which are ionic liquids at room-temperature (RTILs) and being able to support desorption/ionization of the test analytes. As test sample the tryptic peptide/glycopeptide mixture of bovine  $\alpha$ 1-acid-glycoprotein (AGP) was chosen. Bovine AGP has five glycosylation sites; all these *N*-linked glycans belong to the complex type with terminal sialic acid (SA) residues. In an attempt to optimize the ionization conditions and to obtain high quality spectra, the effects of sample spot preparation and the addition of complexing additives were investigated. Those ILMs providing best results regarding glycopeptide analysis were selected for further investigations addressing sensitivity, spot-to-spot reproducibility of intensities and extent of in-source and post-source fragmentation of analytes. The sequence coverage obtained by using these ILMs was compared to the conventional solid matrices. Additionally, the selected ILMs were investigated with respect to the ionization yield of the neat glycans present in an unseparated mixture with peptides after enzymatic cleavage of the oligosaccharides by PNGase F and tryptic digestion. All measurements were carried out in both, positive and negative ionization mode. The identity of glycopeptide peaks detected in the MS<sup>1</sup> mode was verified by MS/MS analysis.

## **1.2. Ionic liquids**

### **1.2.1. Characteristics of ionic liquids**

The term ionic liquid names a class of compounds being organic or semiorganic salts with melting points below 100 °C. ILs staying liquid at room temperature are termed room-temperature ILs (RTILs). ILs possess a very low vapor pressure, are often highly viscous and have frequently good electrical conductivity. Other properties like high thermal and chemical stability, broad liquid range, low combustibility and favorable solvating properties for a range of polar and non-polar compounds are diverse. Some ILs are immiscible whereas others are miscible with water and a number of organic solvents. All these unique physicochemical properties of ILs depend on the chemical structure of cations and anions as well as which cations are paired with which anions. Typical ILs contain an organic cation based on an imidazolium, pyridinium, ammonium or phosphonium group associated with an inorganic ( $\text{Cl}^-$ ,  $\text{NO}_3^-$ ,  $\text{BF}_4^-$ ,  $\text{PF}_6^-$ ) or organic (such as  $(\text{CF}_3\text{SO}_2)_2\text{N}^-$ ,  $\text{CF}_3\text{CO}_2^-$ ) counter ion. The relationship between the structure of ILs and their physicochemical and solvation properties is not well understood yet. However, general trends can be observed within specific classes of ILs. For example, viscosity increases when increasing the alkyl chain length in 1-alkyl-3-methylimidazolium cations and keeping the anion constant [8]. The same holds with density. The numerous combinations of cations and anions available lead to a large number of ILs with different properties that provide considerable flexibility in the selection of the most suitable pair for a specific chemical application.

### **1.2.2. Applications of ILs in analytical chemistry**

Initially, ILs were applied as non-volatile solvents replacing traditional organic solvents in organic synthesis and catalysis. In the last years the role of ILs has become increasingly important in chemical analysis and today the application of ILs is one of the most rapidly growing areas of research in all fields of analytical chemistry [9]. ILs are applied in electrochemistry, chromatography and

electrophoresis, MS, optical spectroscopy and with chemical sensors. As ILs possess good solvating properties, high conductivity, very low volatility, large electrochemical windows and a good electrochemical stability, they are suitable for many electrochemical applications [10]. Recent research on this field is widespread and examples include the use of ILs as electrolytes, as solvents for electrosynthesis, as material for electrodes or electrochemical sensors [11].

ILs have been used in a variety of separation methods [12, 13], e.g. as stationary phases in gas chromatography (GC) [14, 15] and in liquid chromatography (LC) [16], and as mobile phase additives in high performance liquid chromatography (HPLC) [17]. In capillary electrophoresis (CE), ILs are applied as buffer additives [18] and as coating material [19]. The possibility to introduce chiral groups into ILs opens a wide potential for enantioselective separations. These chiral ionic liquids (CILs) consist either of a chiral cation or a chiral anion or both. CILs were used as stationary phases [20] in chiral GC and as additives in the background electrolyte [21] in chiral CE. Further, ILs have been reported as suitable candidates for the replacement of traditional volatile organic solvents in two-phase liquid/liquid extraction processes [22].

Analytical applications of ILs within MS include their use as MALDI matrices [7, 23-41] or as ion-pairing reagents for trace analyses of anions by electrospray ionization mass spectrometry (ESI-MS) in positive ion mode [42-44].

ILs can be transparent in the ultraviolet (UV) and infrared (IR) spectral regions and in contrast to many other polar organic solvents ILs are weakly coordinating solvents. This property makes ILs interesting for using them as solvents for the study of dissolved metal salts and metal complexes [40, 45, 46]. Other applications of ILs in the field of spectroscopy are their use as a medium for photochemical reactions [47] or for the monitoring of organic reactions by absorption spectroscopy [48]. An example for the application of CILs in this area is their use for the determination of the enantiomeric excess of samples by nuclear magnetic resonance (NMR) spectroscopy [49]. Most of the recent developments in the application of ILs in analytical chemistry in general [9, 50-52] and separation science in particular [12, 13] have been summarized in several reviews.

### **1.3. ILs as matrices for MALDI-MS**

Since its introduction by Hillenkamp and Karas in the late 1980s [53], MALDI-MS has become one of the most commonly used techniques for the investigation of biomolecules such as peptides, proteins, oligosaccharides and oligonucleotides. Other application fields of MALDI-MS include the analysis of small organic molecules (including amino acids, lipids and sugars) [54] and technical polymers [41]. As a new application of MALDI-MS, the imaging of tissues has been developed [55]. The formation of mainly singly charged analyte ions by MALDI supports the possibility of multiplexed analyses and the relatively easy interpretation of the obtained spectra. Furthermore MALDI-MS provides other benefits like high sensitivity, low sample consumption, fast and simple sample preparation and a moderate tolerance against contaminations, such as salts and detergents. Therefore, MALDI-MS has become an important tool for proteomics [56] and glycomics [35, 57].

#### **1.3.1. The role of the matrix in the MALDI process**

The basic principle of MS is the separation of ions according to their mass-to-charge ( $m/z$ ) ratio. In the MALDI process the energy necessary for ionization and desorption of the analyte is supplied by a laser pulse. In MALDI-MS a mixture consisting of the analyte and a UV- or IR-absorbing matrix, respectively, is irradiated by a pulsed laser of the wave length corresponding to the absorption region of the matrix [53]. This irradiation induces an ionization/desorption process of analyte and matrix molecules. The mechanism of the MALDI ionization process itself is complex and not in all details understood yet. In this process the matrix has the role to absorb the laser energy at the laser wavelength used without transferring excessive internal energy to the analyte, while promoting the desorption of the analyte as well as its ionization (by protonation or deprotonation). The choice of matrix has a profound impact on the ionization yield, the formation of adducts and the stability (or fragmentation) of the analyte. The selection of matrix thus influences the relative abundance of analytes, intensities, fragmentation of the analytes and the types of analyte ions detectable.

Conventional MALDI matrices are solids like sinapinic acid, CHCA and DHB, and rely on the co-crystallization of matrix and analyte molecules.

### **1.3.2. The introduction of ILs as MALDI matrices**

Despite the widespread application of MALDI-MS in many analytical areas, some major short-comings still remain. One weak point of MALDI-MS is the analyte size and/or type restriction of conventional crystalline matrices. Matrices that are suitable for one class of analytes may be unsuitable for another class even though they may have a similar molecular weight range. Therefore, a large number of different matrix substances have been used for various applications and it is difficult to select appropriate matrices for each sample. Another problem associated with solid matrices is the formation of so called “hot spots” which leads to inhomogeneous sample preparations which causes a significant variation of signal intensities between different spots of the same preparation and even between different shot-locations within the same spot [58]. This shot-to-shot and spot-to-spot variance is one of the major factors limiting the application of MALDI-MS for quantitative analysis, demands enhanced repetition numbers of measurements and complicates automated measurements. To yield better performances in terms of reproducibility, sensitivity, resolution and dynamic mass range several approaches have been developed concerning both sample preparation and choice of matrix, e.g., fast evaporation methods [59] or the addition of co-matrices, mainly small carbohydrates such as fructose or fucose [60].

An alternative approach to overcome the short-comings of commonly used solid matrices is their replacement by ILs. The requirements to make ILs possible candidates for MALDI matrices are properties including vacuum-stability, chemical inertness, and the ability to generate a homogeneous matrix/analyte mixture. They must be able to absorb the laser energy at the laser wavelength used and should conduct the desorption/ionization process without transferring excessive internal energy to the analyte.

UV light-absorbing ILs as suitable non-volatile MALDI-matrices were first introduced by Armstrong et al. in 2001 [7]. This new class of ILs was called ionic liquid matrices (ILMs or class II ionic liquids), being organic salts created by the dissolution of

commonly used crystalline MALDI matrices, like CHCA, DHB or sinapinic acid, in a volatile solvent together with organic bases as counter ions, like tributylamine, pyridine or 1-methylimidazole. Some of the new synthesized ILs were successfully tested for analyzing proteins, peptides and polyethylene glycols (PEGs). The results obtained by using these new ILMs were found being equal or even improved when compared with their solid analogues when considering sensitivity and spot-to-spot reproducibility. Accordingly, the applications of ILMs have been reported in a number of publications.

### **1.3.3. Sample homogeneity in ionic liquid matrices**

One of the most determining arguments for the application of ILs is the sample homogeneity available in these matrix systems. ILMs, even at room temperature solid ILs, form smooth, homogeneous surfaces in contrast to the classical matrices that display crystallization and numerous shapelessness [7]. They exhibit a more uniform distribution of analyte and matrix compared to generally applied matrices [7, 31, 36, 61, 62]. Furthermore, in solid matrices the formation of “hot spots” has the effect that frequently low or no analyte signals can be found at several positions of the preparation, whereas high signals are found at other positions. This effect was reported to be dramatically reduced by the application of ILMs leading to an enhanced spot-to-spot and shot-to-shot reproducibility [34, 62]. As a second aspect, liquid preparations using ILMs were found to provide a stable ion signal production for an extended number of shots on one constant sample position [31, 36]. This factor may be useful for MALDI-MS experiments requiring a high number of repetitive shots such as MS/MS analyses.

### **1.3.4. Substances which can be analyzed in ILMs**

A variety of substance classes including the whole range of organic analytes and biopolymers have been analyzed in ILMs. In addition to the most commonly investigated polymeric biomolecules like proteins [15, 23, 25] [31] and peptides [15, 23, 26, 29, 34, 36, 38, 63], many other analytes like glycopeptides [26, 37], glycans



[31, 37], polysaccharides like pullulans [33], polynucleotides [24, 29], lipids [23], phospholipids [23, 30], sulfolipides [64], synthetic polymers [15, 23, 25, 31, 41], sugars [23, 25, 26, 28, 62], sulfated carbohydrates [26, 27, 35, 65], glycolipids [31], vitamins [62] and low molecular weight compounds like amino acids [23, 62] were measured using these matrices. Similar to traditionally used crystalline matrices, up to now there have been no definite rules for prognosting the qualification of an ILM for the measurement of a specific compound. For this reason, as common for the crystalline matrices, before measuring a specified new class of analytes suitable ILMs have to be found by testing a set of matrices.

### **1.3.5. Sensitivity and adduct formation in ILMs**

There are several key criteria arguing for or against the application of a specific MALDI matrix: sensitivity, mass accuracy and achievable resolution. Other factors that have to be considered are the stability of analytes and the formation of adducts. The comparison of the sensitivity achieved in ILMs and classic crystalline matrices has shown no consistent results in different publications. For example, for the analysis of peptides by using ILMs, comparable or even increased sensitivities were reported by a number of groups in positive [7, 23, 66] and negative ion mode [61], whereas others reported decreased sensitivities [31, 37]. Increased sensitivities were reported for oligonucleotides [24], lipids, oligosaccharides and low molecular weight analytes like amino acids [23]. Summarizing the observations made by several groups, the composition of the ILM can have an critical influence on the sensitivity for a specific analyte, and both the cation and the anion have to be elected with care for attaining optimal ionization yields [24, 38]. Recently, a new approach was introduced by J. A. Crank and D. W. Armstrong [25]. They developed numerous new ILMs by systematically varying the anionic and cationic moieties and tested more than 100 cation/anion pairs by measuring proteins, peptides and carbohydrates to find an ILM with best physical properties, analyte signal intensities and widest mass detection range. The authors observed that both proton affinity and  $pK_a$  of the cation have a major effect on the ability of ILMs to effectively ionize analytes. The sensitivity available can further be influenced by the formation of adducts with sodium and potassium ions and matrix cations, which results in a significant

decrease of protonated ion signal intensities [31]. Many ILMs show a strong tendency to generate increased formation of sodium and potassium adducts [7, 25, 38]. The formation of such alkali adducts splits the analyte signal into several peaks complicating thereby the spectra and diminishing the signal intensities and thus sensitivity. This might be a problem for instance in peptide mass fingerprint based identification of proteins. The formation of sodium and potassium adducts can, to a certain extent, be suppressed by the addition of acids like trifluoroacetic acid (TFA). For the application of CHCA-based ILMs also ammonium phosphate can be added to suppress adduct formation [36]. Adducts of the analytes with matrix compounds have not yet been described to cause problems. E.g., when investigating pullulans by the use of the ILM butylammonium 2,5-dihydroxybenzoate (BuA-DHB) the principal ions detected were butylammonium adducts [33].

A notable advantage of several ILMs is the absence of matrix peaks generated by conventional matrices, which makes them suitable matrices for the analysis of samples in the lower mass region such as amino acids, lipids and oligosaccharides [23].

### **1.3.6. Fragmentation of analytes**

A major factor for characterizing the quality of a matrix is the stability of the analyte ions formed. With MALDI-MS, in-source and post-source decay (ISD and PSD) of labile structures is commonly taking place, leading for instance to a loss of  $\text{NH}_3$  from the peptide backbone or the loss of phosphoric acid attached to Serine and Threonine or to the cleavage of SAs attached to glycans. The extent of fragmentation depends on the amount of internal energy the analytes received during the ionization/desorption process in the ion-source. The internal energy of analytes is influenced by the constitution of the matrix, the acceleration voltages applied and the laser energy.

The slightly lower laser energies [23, 25, 41] required when using ILMs might be one reason for the decreased extent of fragmentation observed for different types of analytes. For example, a lower extent of fragmentation (loss of  $\text{SO}_3$  and SAs from sulfated and sialylated oligosaccharides, respectively) was found with the ILM tri(*N,N,N',N'*-tetramethylguanidinium) *p*-coumarate compared to measurements

using conventional CHCA [26]. Similar observations were made analyzing sialylated [31] and sulfated sugars [28] comparing the ILM BuA-DHB to pure DHB. A lower extent of fragmentation through the loss of  $\text{SO}_3$  of underivatized polysulfated, polycarboxylated oligosaccharides was found when using the ILM di(*N,N,N',N'*-tetramethylguanidinium)  $\alpha$ -cyano-4-hydroxycinnamate [28]. The loss of phosphoric acid frequently observed for phosphorylated peptides was not reduced in ILMs [34]. Minimized polymer degradation by means of ILMs could also be obtained when analyzing labile polar polymers [41] and pullulans [33]. Therefore, the use of ILMs can lead to an improved analysis of labile analytes caused by the decrease of fragmentation in MALDI-MS. In future research it will be necessary to address this behavior in more detail.

Another important aspect is the hydrolysis of acid labile analytes, mainly of oligosaccharides. Aqueous solutions of conventional MALDI matrices exhibit strongly acidic pH values. In contrast, ILMs obtain relatively moderate pH values when mixed with the aqueous sample solution. Therefore, the use of ILMs reduces the risk of on-target decay by acidic hydrolysis of acid labile bindings [31].

### **1.3.7. Quantitative analysis**

Prior to the introduction of ILMs, MALDI-MS was regarded to be completely unsuitable for quantitative analysis because of following aspects: First, due to the competitive nature of the ionization process in an analyte mixture ion signal intensities depend not only on the quantity of the analyte but also on quality and quantity of other compounds present in the sample. Ion suppression effects are commonly observed in MALDI-MS depending on the chemical composition of the analytes, e.g., on the amino acid sequence in the case of peptides. Secondly, the above mentioned “hot spot” formation, when using conventional crystalline matrices, leads to poor shot-to-shot and spot-to-shot reproducibility.

It was shown by some authors that the application of ILMs enable an improved relative quantification of low molecular weight compounds like amino acids and sugars [62], and small proteins, peptides and oligonucleotides [29.] compared to conventional matrices. The use of ILMs together with an increased matrix-to-analyte ratio permits a quantification of peptides without the use of internal standards [34].

The large influence of the matrix-to-analyte ratio on the range of linearity prevents the application of the method for those analyses in which the orders of magnitude of analyte's concentration are unknown, e.g. for a direct quantification of peptides in a proteomics environment. On the other hand, in case of enzyme reactions, the starting concentrations of the substrates are generally known. Therefore the method is applicable for monitoring enzymatic reactions (enzyme screening) [34]. Another interesting approach is the direct MALDI-screening of enzyme-catalyzed reactions performed in ILMs which serve as co-solvent for the enzymatic reaction as well as the matrix for the direct monitoring [31].

### **1.3.8. MALDI imaging**

MALDI imaging has emerged as a powerful tool for the direct detection of biomolecules, mainly phospholipids, proteins and peptides, in tissue samples [55]. The performance of such experiments allows a simple subcellular localization of biomolecules without time consuming and complex sample preparation steps. Nevertheless, this method is still challenging due to the complexity of the sample and still needs technical innovations. As new approach several ILMs were tested for the improvement of direct tissue analysis by MALDI imaging [61]. The dissolved ILMs formed by combination of CHCA with aniline, pyridine and di- or triethyl amine were directly applied onto frozen tissue slices by pipetting. Compared to conventional crystalline CHCA, the use of ILMs, especially aniline-CHCA, was shown to obtain higher sensitivity, increased mass accuracy and improved peak resolution of the images. Reduced fragmentation led to higher signal intensities of the precursor ions and therefore, to improved direct on-tissue PSD analysis. Furthermore, ILMs were also shown to obtain increased sensitivities in negative ion mode making them useful for the analysis of negatively charged analytes such as phospholipids. Recently, the ILM 1-methylimidazolium-CHCA was investigated for MALDI imaging of gangliosides [67]. One major drawback for imaging gangliosides in tissue using conventional MALDI matrices is that sialic acid residues can be dissociated easily during the desorption/ionization process. This problem could be reduced significantly by the application of ILMs. The conclusion of these studies is that the use of ILMs is beneficial for improved direct tissue analysis by MALDI imaging.

## **2. Experimental**

### **2.1. Materials**

Bovine  $\alpha$ 1-acid-glycoprotein (AGP), PNGase F (recombinant from *Chryseobacterium meningosepticum*), trypsin (from porcine pancreas, proteomics grade, modified), iodoacetamide, *N,N*-diisopropylethylamine (DIEA) ( $\geq 99.5\%$ ) and trifluoroacetic acid (TFA), were obtained from Sigma-Aldrich (St. Louis, MO, USA).

$\alpha$ -Cyano-4-hydroxycinnamic acid (CHCA) ( $\geq 99\%$ ), 2,4,6-trihydroxyacetophenone (THAP) ( $\geq 99\%$ ), hexylamine (HxA) ( $\geq 99.5\%$ ), butylamine (BuA) ( $\geq 99.5\%$ ), *N,N,N',N'*-tetramethylguanidine (TGM) ( $\geq 99\%$ ), 2,5-Dihydroxybenzoic acid (DHB) ( $\geq 99\%$ ), di-ammonium hydrogen citrate (AC) ( $\geq 99\%$ ), di-ammonium hydrogen phosphate (AP) ( $\geq 99\%$ ), dithiothreitol (DTT) ( $\geq 99\%$ ), ammonium hydrogen carbonate ( $\geq 99\%$ ) and methanol ( $\geq 99.9\%$ ) were purchased from Fluka (Buchs, Switzerland); guanidinium chloride and acetonitrile from Merck (Darmstadt, Germany), and tris-(hydroxymethyl)-aminomethan hydrochloride (TRIS-HCl) from Carl Roth (Karlsruhe, Germany).

PD-10 desalting columns pre-packed with Sephadex G25 were purchased from GE Healthcare (Uppsala, Sweden).

Water of ultra high quality (UHQ) was prepared by an Elgastat UHQ apparatus (Elga LabWater, Siershahn, Germany).

### **2.2. Sample preparation**

A measured quantity of 7.5 mg of bovine AGP (about 100 nmol) was dissolved in 1.2 mL of denaturing buffer (6-M guanidinium chloride in 500-mM TRIS-HCl, pH adjusted to 8.5 with 2 M NaOH). To reduce the disulfide bonds 6.7  $\mu$ L of 0.5 M DTT in water were added followed by 1 h of incubation at 37 °C. After cooling down to room temperature alkylation was performed by the addition of 60  $\mu$ L of 2 M iodoacetamide in denaturing buffer and incubating the solution for 1 h in the dark. Afterwards, excess reagents and buffer salts were removed with PD-10 size-exclusion columns

using water for elution. After addition of 390  $\mu\text{L}$  of 0.5 M ammonium hydrogen carbonate buffer at pH 7.8 and 60  $\mu\text{g}$  trypsin the digestion was done by overnight incubation at 37  $^{\circ}\text{C}$ . On the next day, the digest was divided into aliquots of 110  $\mu\text{L}$  (0.24 mg digested protein), evaporated in a speed-vac centrifuge and stored at -25  $^{\circ}\text{C}$ .

To remove *N*-glycans from bovine AGP the tryptic digest was treated with PNGase F. The enzyme was, as per manufacturer's manual, dissolved in 100  $\mu\text{L}$  UHQ water yielding 500 units/mL. This resulted in an enzyme solution containing 5 mM potassium phosphate buffer at pH 7.5. Then an aliquot corresponding to 0.24 mg tryptic digested bovine AGP was dissolved in 195  $\mu\text{L}$  UHQ water and 20  $\mu\text{L}$  of the enzyme solution was added. Digestion was carried out by overnight incubation at 37  $^{\circ}\text{C}$ . The resultant digest was portioned in 3 aliquots, lyophilized and stored at -25  $^{\circ}\text{C}$ .

### **2.3. Preparation of the ionic liquids**

To a solution of CHCA (100 mM), THAP or DHB (both 200mM) in methanol, an equimolar amount of DIEA, BuA, HxA or TMG was added and shaken at room temperature for 1 min. After this, methanol was removed in a vacuum evaporator. Subsequently, the ILs were redissolved in methanol to a concentration of 50 to 400 mg/mL. The ILs were prepared freshly and used within several hours.

### **2.4. Matrix solutions and sample preparation for MALDI-MS analysis**

MALDI sample preparation was performed using standard stainless steel targets and applying the dried droplet technique. The matrix/analyte solutions on the MALDI target were allowed to dry at room temperature, afterward the preparation was immediately transferred into the MALDI-MS instrument.

#### THAP as solid matrix

0.5  $\mu\text{L}$  of AC (50 mg/mL in 0.1% TFA in water) was deposited on a MALDI target and mixed with 1  $\mu\text{L}$  aqueous sample solution (200 pmol/ $\mu\text{L}$ ). Immediately thereafter, a volume of 1  $\mu\text{L}$  of matrix solution (25 mg/mL THAP in methanol) was added.

#### CHCA and DHB as solid matrices

1  $\mu\text{L}$  aqueous sample solution (200 pmol/ $\mu\text{L}$ ) was applied onto the target and mixed with 1  $\mu\text{L}$  matrix solution (10 mg CHCA per mL and 20 mg DHB per mL, both in 50% aqueous acetonitrile in 0.1% TFA).

#### ILs as ILMs

For their first applications as MALDI matrices the freshly prepared ILs (DIEA-CHCA, BuA-CHCA, HxA-CHCA, TGM-CHCA, DIEA-THAP, BuA-THAP, HxA-THAP, TGM-THAP, DIEA-DHB, BuA-DHB, HxA-DHB and TGM-DHB) were dissolved in methanol to a concentration of about 400 mg/mL. For MALDI sample preparation 1  $\mu\text{L}$  aqueous sample solution (200 pmol/ $\mu\text{L}$ ) was placed on the target and the same volume ILM solution was added, and proper mixing of matrix and sample was achieved by repeated pipetting up and down the mixture.

#### Room-temperature ILs as ILMs

For assessing optimal amounts of ILM deposited per spot the following RTILs, DIEA-CHCA, TGM-CHCA, DIEA-THAP, BuA-THAP, HxA-THAP, TGM-THAP, BuA-DHB and HxA-DHB, were tested with concentration ranges from 50 to 400 mg/mL in methanol. Using a volume of 1  $\mu\text{L}$  sample solution (200 pmol/ $\mu\text{L}$ ) and mixing with the same volume of matrix solutions on the target, final amounts of 50, 100, 150, 200, 300 and 400  $\mu\text{g}$  RTIL, respectively were deposited per spot.

#### AC as ILM solution additive

With intent to increase the spectra quality the stock solutions of TMG-THAP (100 mg/mL) and Bu-DHB (150 mg/mL) in methanol were mixed with a solution of AC (50 mg/mL in 0.1% TFA in water) in a ratio of 2:1 (v/v) to a final concentration of 70 mM. For MALDI analysis 1  $\mu\text{L}$  sample solution (200 pmol/ $\mu\text{L}$ ) was deposited on the target and mixed with 1.5  $\mu\text{L}$  ILM/AC solution.

### AP as ILM solution additive

The effect of AP concentration on the spectrum quality when using ILMs was investigated as follows. The stock solutions of DIEA-CHCA, TGM-CHCA, BuA-DHB, HxA-DHB (all four 200 mg/mL in methanol), DIEA-THAP, BuA-THAP, HxA-THAP and TGM-THAP (all four 150 mg/mL in methanol) were diluted with a AP solution (10 or 100 mM in pure water) in a ratio of 3:1 (v/v) to a final concentration of 2.5 mM and 25 mM, respectively. For MALDI measurements a volume of 1  $\mu$ L sample solution (200 pmol/ $\mu$ L) was placed on the target and mixed with 1.3  $\mu$ L of each ILM/AP solution.

### Determination of sensitivity and spot-to-spot reproducibility with ILMs in comparison to solid THAP

Limit of detection (LOD) and the reproducibility of signal intensity values were determined for selected compounds in the sample mixtures. These measurements were done with TMG-THAP (150 mg/mL in methanol diluted with 100 mM AP solution in water in a ratio of 3:1 (v/v)), BuA-THAP (150 mg/mL in methanol diluted with 10 mM AP solution in water in a ratio of 3:1 (v/v)), DIEA-CHCA (200 mg/mL in methanol diluted with 100 mM AP solution in water in a ratio of 3:1 (v/v)) and the solid THAP. For the determination of LOD values the sample solutions were diluted with water to concentrations from 100 pmol to 1 fmol. For the determination of the spot-to-spot reproducibility of peak heights spectra were acquired from seven different spots containing the same amounts of analytes (100 pmol/ $\mu$ L). In all cases, a volume of 1  $\mu$ L sample solution was deposited on the target and mixed with 1.3  $\mu$ L of the respective ILM/AP solution. THAP was applied as described before.

## **2.5. Mass spectrometry**

MALDI-MS and MALDI-MS/MS experiments with low-energy collision-induced dissociation (CID) were performed on an AXIMA-QIT instrument (Shimadzu Biotech - Kratos Analytical, Manchester, UK). This hybrid-instrument consists of a 3D quadrupole ion trap (QIT) coupled to a reflector time-of-flight mass analyzer (rTOF). The instrument is equipped with a pulsed nitrogen laser (wavelength of 337 nm) operating with a pulse width of about 4 ns. Ions were accelerating from the target by applying a voltage of  $\pm$  4 kV. The trapped ions were cooled by flooding the QIT



continuously with helium at a high vacuum condition of  $5 \times 10^{-5}$  mbar. To additionally support the ion-cooling process, a short pulse of argon was injected into the QIT immediately before the ion introduction. CID was carried out by applying an additional pulse of argon directly before the radio frequency-induced precursor ion excitation. Mass spectra were obtained under the following settings: The laser power applied was slightly above the threshold energy required for obtaining desorption/ionization. Measurements were executed in both, positive and negative, ionization mode and using both mass ranges provided by the ion trap, *i.e.*, instrument setting “Mid” aimed for masses from 700 Da upward and “High” for masses above 2000 Da. All MS<sup>1</sup> spectra were constituted from an average of several hundred profiles composed of the accumulation of two single laser shots. CID spectra were acquired by averaging 1000-2000 profiles composed of the accumulation of two single laser shots using a precursor ion selection width of 1/70, 1/250, or 1/1000 of the precursor ion mass in MS<sup>2</sup>. Spectra were not smoothed. External calibration was carried out using a mixture of fullerenes (Kratos Analytical). Acquisition and data processing were managed by Launchpad software (version 2.7.2.; Kratos Analytical).

## **3. Results and Discussion**

### **3.1. Ionic liquid matrices**

#### **3.1.1. Properties of the investigated ionic liquids**

Twelve ILs covering three different anions and four different cations were prepared and tested for suitability as ILMs in MALDI-MS. (Abbreviations of prepared ILs are given in Table 3.1; structures of their acidic and basic compounds are shown in Figs. 4.1 and 4.2.) As anions three commonly used and successful MALDI matrices were selected, *i.e.*, CHCA, DHB and THAP, and the four cations covered amines with different  $pK_a$  values and proton affinities, *i.e.*, the two primary amines BuA ( $pK_a=10.8$ ) and HxA ( $pK_a=10.6$ ), the secondary amine DIEA ( $pK_a=11.4$ ), and the very basic TMG ( $pK_a=13.6$ ).

To avoid the need for appropriate co-crystallization of matrix and analyte, a typical requirement for crystalline matrices, and to overcome inhomogeneous analyte distribution, the focus was given on matrices which are ionic liquids at room-temperature (RTILs). The criteria for selection of appropriate ILMs were consequently, that the organic ion pair (salt) should stay liquid at room temperature and can support desorption/ionization of the test analytes. Eight of the twelve ILs investigated here formed colourless to yellowish uniform liquid spots when applied onto the MALDI stainless steel target after evaporation of the solvent. The other four ILs (BuA-CHCA, HxA-CHCA, TMG-DHB and DIEA-DHB) formed thin solid layers on the target under room temperature conditions.

To assess the efficiency of the ILs to assist desorption/ionization of analytes all ILs have been tested using the tryptic digest of bovine AGP as test-sample. All ILMs except the solid TGM-DHB showed analyte signals for peptides in the positive ion mode (Table 3.1).

All further investigations were carried out with those ILs staying liquid at room temperature, assuming that the liquid nature of RTILs might provide potential advantages over the solid state of the commonly used crystalline matrices.

**Table 3.1:** ILs used as matrices for MALDI-MS and specification of their physical state on the target after evaporation of the solvent as well of their ability to support the MALDI process for peptide analytes

<b>Ionic liquid</b>	<b>Abbreviation</b>	<b>Physical state</b>	<b>Analyte signal</b>
<i>N,N,N',N'</i> -tetramethylguanidinium $\alpha$ -cyano-4-hydroxycinnamate	TMG-CHCA	liquid	+
butylammonium $\alpha$ -cyano-4-hydroxycinnamate	BuA-CHCA	solid	+
hexylammonium $\alpha$ -cyano-4-hydroxycinnamate	HxA-CHCA	solid	+
<i>N,N</i> -diisopropylethylammonium $\alpha$ -cyano-4-hydroxycinnamate	DIEA-CHCA	liquid	+
<i>N,N,N',N'</i> -tetramethylguanidinium 2,4,6-trihydroxyacetophenone	TMG-THAP	liquid	+
butylammonium 2,4,6-trihydroxyacetophenone	BuA-THAP	liquid	+
hexylammonium 2,4,6-trihydroxyacetophenone	HxA-THAP	liquid	+
<i>N,N</i> -diisopropylethylammonium 2,4,6-trihydroxyacetophenone	DIEA-THAP	liquid	+
<i>N,N,N',N'</i> -tetramethylguanidinium 2,5-dihydroxybenzoate	TMG-DHB	solid	-
butylammonium 2,5-dihydroxybenzoate	BuA-DHB	liquid	+
hexylammonium 2,5-dihydroxybenzoate	HxA-DHB	liquid	+
<i>N,N</i> -diisopropylethylammonium 2,5-dihydroxybenzoate	DIEA-DHB	solid	+

### 3.1.2. ILM spot preparation: applied amount of ILM and film shape

Sample spot preparation is known to have significant impact on the efficiency of MALDI processes when dealing with solid matrices. It has also been observed that the quantity of the ILM deposited per spot had a considerable impact on the quality of

the spectra obtained and on the signal-to-noise (S/N) ratio achieved. Thus, the efficiency of RTILs was tested applying different amounts of ILMs onto the target yielding a different layer thickness. For this purpose, the same amount of analyte (200 pmol tryptic digest of bovine AGP) was analyzed using IL-amounts between 50 and 400 µg per spot (spot radius about 3.5 mm). The ranges in which the best spectra quality was obtained are shown for each ILM in Table 3.2. When applying amounts within these ranges, all analyte/matrix mixtures formed a thin planar film on the target after evaporation of the solvent. There are only two exceptions, namely BuA-THAP and HxA-THAP, which contracted to small single drops or a ring, probably due to their high viscosity and/or surface tension.

**Table 3.2:** Amount of ILM per spot found as being optimal for the application as MALDI-matrix and the form of the analyte/matrix layer on the target.

<b>ILM</b>	<b>optimal ILM-quantity per Spot</b>	<b>form of the analyte/matrix layer</b>
<b>TMG-CHCA</b>	50-400 µg	film
<b>DIEA-CHCA</b>	200 µg	film
<b>TMG-THAP</b>	50-200 µg	film
<b>BuA-THAP</b>	100-200 µg	drops or ring
<b>HxA-THAP</b>	100-200 µg	drops or ring
<b>DIEA-THAP</b>	150 µg	film
<b>BuA-DHB</b>	>200 µg	film
<b>HxA-DHB</b>	>200 µg	film

## 3.2. Molecular Ions observed with ILMs

### 3.2.1. Molecular Ions formed in ILMs:

The spectra obtained with all ILMs investigated here showed a high extent of formation of multiple sodium adducts when dealing with peptides and glycopeptides in the positive as well as in the negative ionization mode. In addition to the molecular ions  $[M+H]^+$  and  $[M-H]^-$ , being the predominant ions when using the solid matrices, the sodiated ions  $[M+Na]^+$ ,  $[M-H+2Na]^+$ ,  $[M-2H+3Na]^+$  and  $[M-3H+4Na]^+$  were formed with high intensities in the positive mode and the ions  $[M-2H+Na]^-$ ,  $[M-3H+2Na]^-$  and

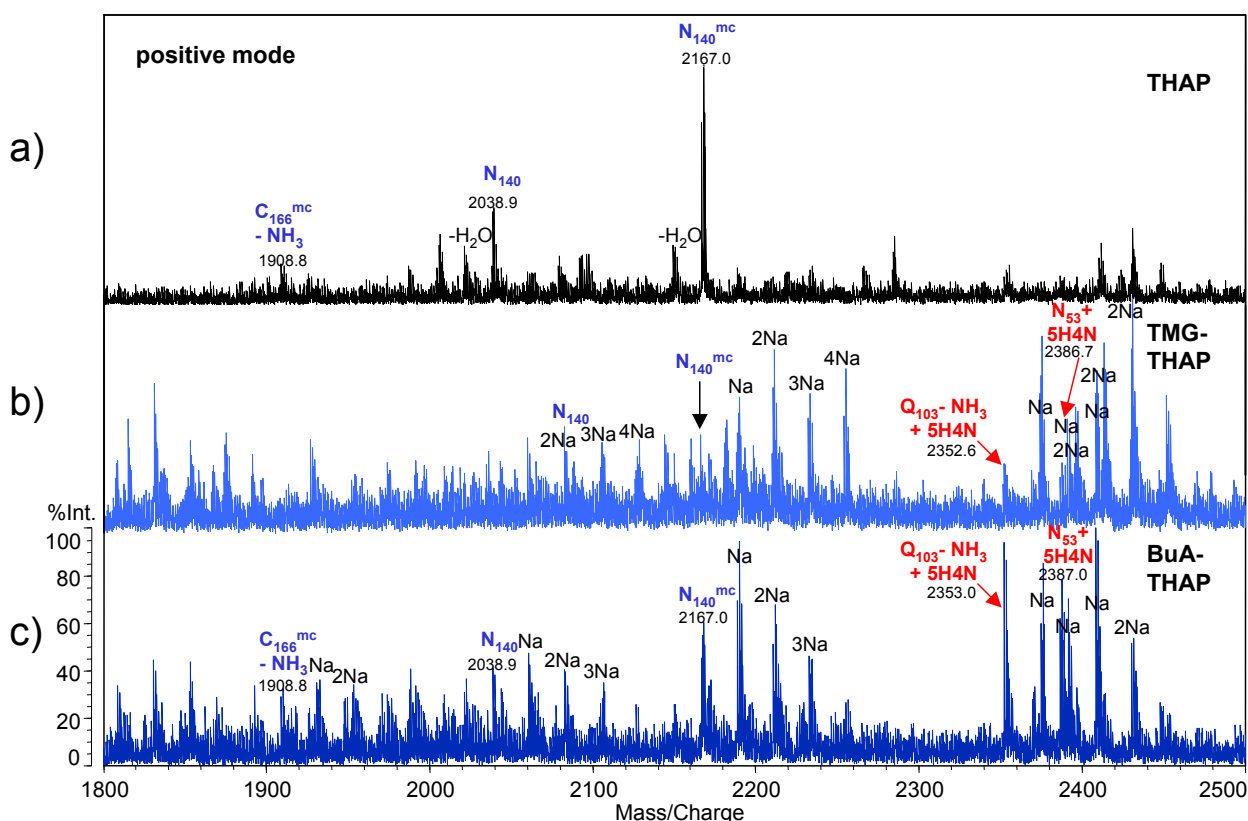


**Figure 3.1:** Molecular ions formed in ILMs in comparison to crystalline matrix: MALDI-QIT-rTOF mass spectra of an unseparated tryptic digest of bovine AGP in the positive ion mode obtained by using (a) THAP as solid matrix; (b) TGM-THAP as ILM; and (c) BuA-THAP as ILM. Numerical values specify the monoisotopic masses of the  $[M+H]^+$  ions; n Na indicates the ion  $[M-(n-1)H+nNa]^+$ . Tryptic peptides are specified by the first amino acid in the one letter code and its sequence number; mc stands for the presence of a missed cleavage site.

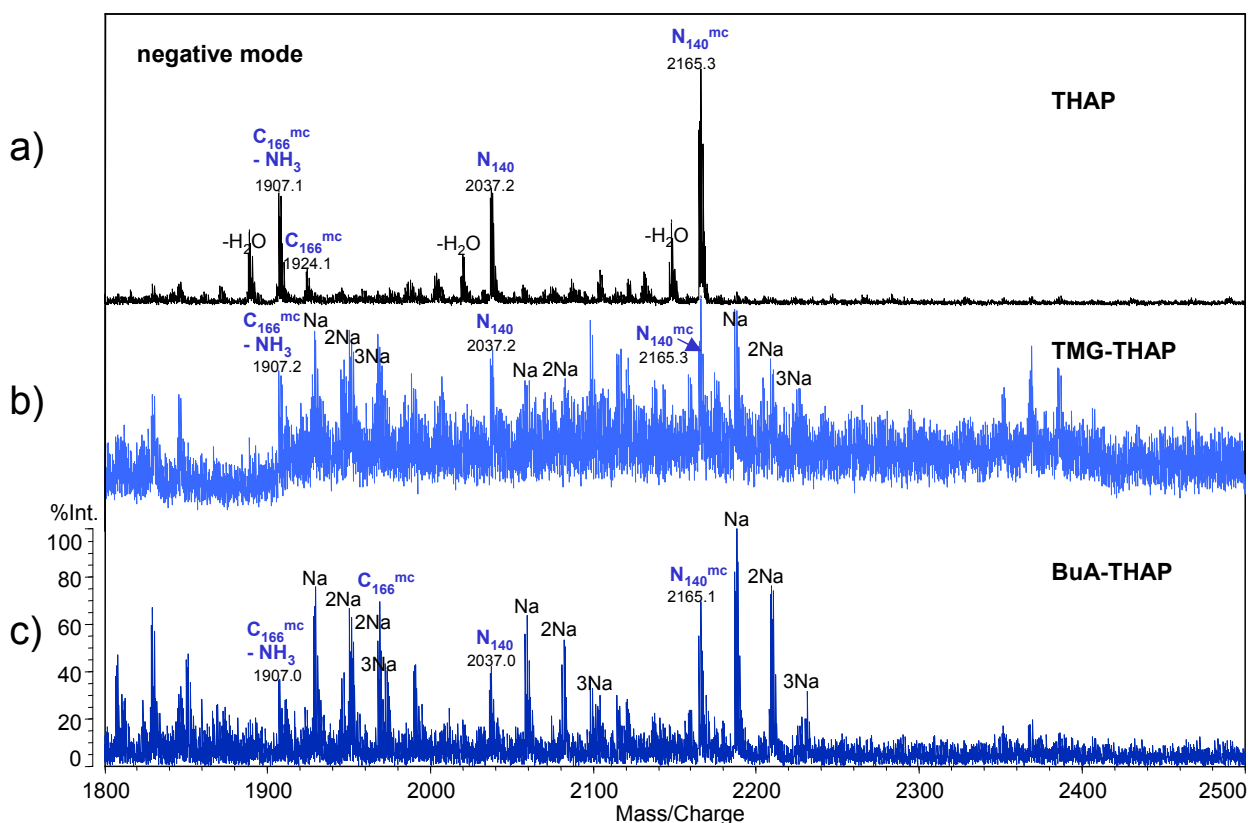


**Figure 3.2:** Molecular ions formed in ILMs in comparison to crystalline matrix: MALDI-QIT-rTOF mass spectra of an unseparated tryptic digest of bovine AGP in the negative ion mode obtained by using (a) THAP as solid matrix; (b) TGM-THAP as ILM; and (c) BuA-THAP as ILM. Numerical values specify the monoisotopic masses of the  $[M-H]^-$  ions; n Na indicates  $[M-(n+1)H+nNa]^-$ . Abbreviations (abbr.) as specified in Fig. 3.1.

$[M-4H+3Na]^-$  in the negative mode when using the ILMs. This effect is illustrated in the Figs. 3.1 and 3.2 by exemplary spectra showing the differences in molecular ion formation between ILMs (TMG-THAP and BuA-THAP) and THAP. The enhanced formation of multiple sodium adduct peaks split the signal intensities of the analytes into several peaks complicating thereby the spectra and decreasing sensitivity and S/N-ratio, respectively.

It should be mentioned that the results gained with THAP were the best when comparing spectra obtained by the three crystalline matrices CHCA, DHB and THAP. With CHCA, good spectra could be obtained only for the lower mass range up to  $m/z = 2000$  and with DHB the number of peptide peaks attained was very low.

### 3.2.2. Effect of complexing additives on molecular ion formation

#### 3.2.2.1. Di-ammonium hydrogen citrate as ILM solution additive

With the intent to improve the quality of the spectra obtained by using ILMs, di-ammonium hydrogen citrate (AC) was added to TGM-THAP and BuA-DHB, to a final concentration of 70 mM. These solutions were tested as ILMs in the positive ionization mode, again measuring the tryptic digest of bovine AGP. In contrast to our expectations based on previous experiences with the crystalline matrix THAP, no improvement concerning a reduced formation of sodium adduct peaks could be observed. With TMG-THAP/AC there was a little decrease of sodium adduct formation leading to a clearer spectrum in the lower mass range only, in the high molecular mass range the noise became significantly enhanced (Fig. 3.3). With BuA-DHB no effect on adduct formation could be noticed at all (Fig. 3.4).

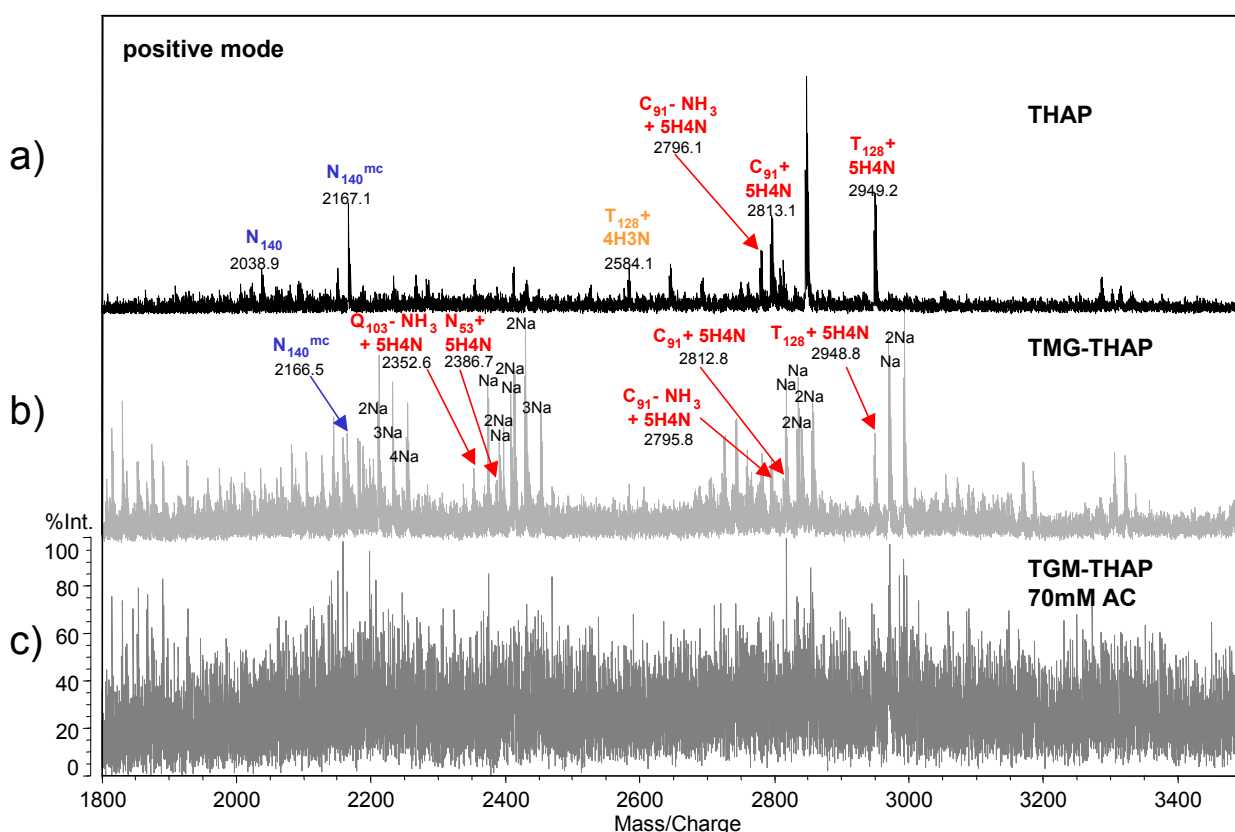


**Figure 3.3:** MALDI-QIT-rTOF mass spectra of an unseparated tryptic digest of bovine AGP in the positive ion mode obtained by using (a) THAP as solid matrix; (b) TGM-THAP (without adding AC) as ILM; and (c) TGM-THAP adding AC to a final concentration of 70 mM as ILM. Numerical values specify the monoisotopic masses of the  $[M+H]^+$  ions; n Na indicates the ion  $[M-(n-1)H+nNa]^+$ . H stands for Hexose (Hex); N for N-acetyl-D-glucosamine (GlcNAc); other abbr. as specified in Fig. 3.1.

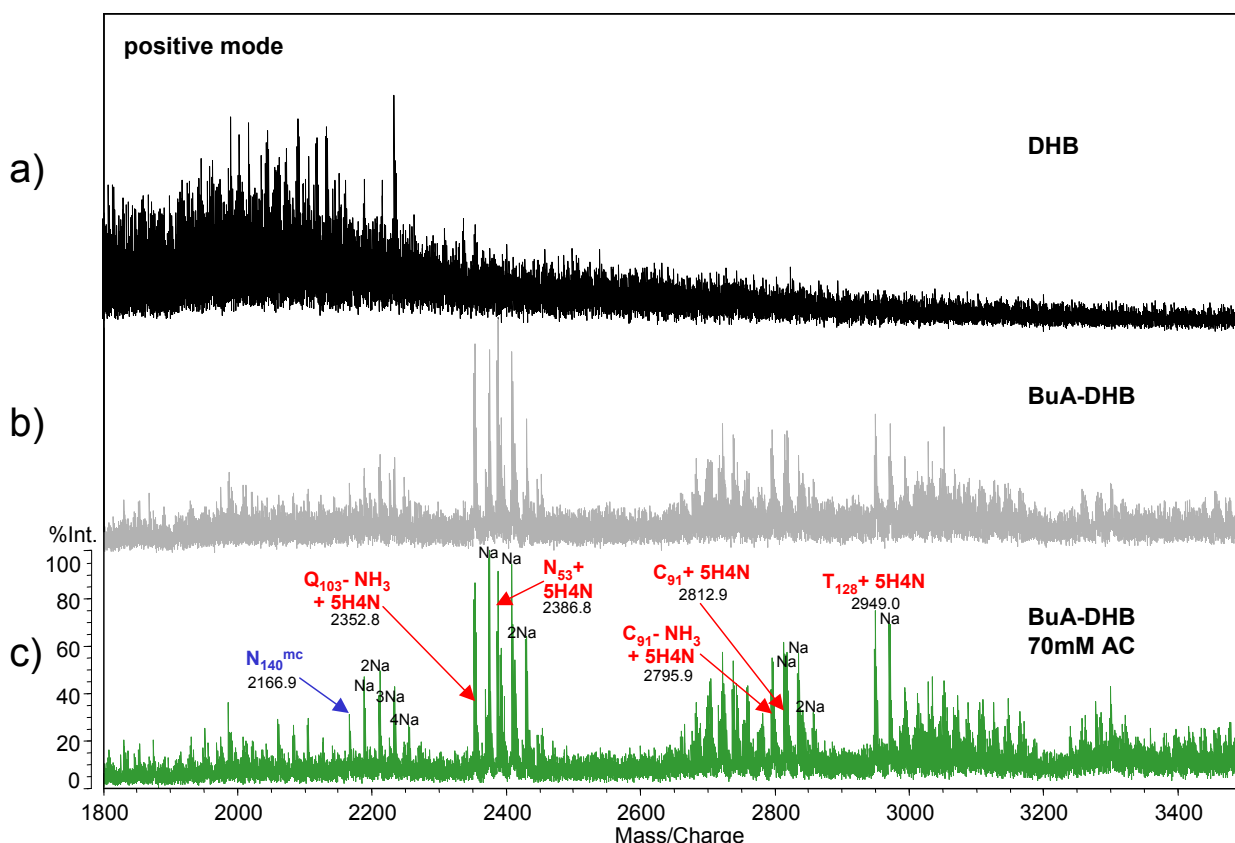


**Figure 3.4:** MALDI-QIT-rTOF mass spectra of an unseparated tryptic digest of bovine AGP in the positive ion mode obtained by using (a) DHB as solid matrix; (b) BuA-DHB (without adding AC) as ILM; and (c) BuA-DHB adding AC to a final concentration of 70 mM AC as ILM. Numerical values specify the monoisotopic masses of the  $[M+H]^+$  ions; n times Na indicates the ion  $[M-(n-1)H+nNa]^+$ . H stands for Hex; N for GlcNAc; other abbr. as specified in Fig. 3.1.

#### 3.2.2.2. Di-ammonium hydrogen phosphate as ILM solution additive

Following a method previously applied for CHCA based ILMs [36] it was attempted to reduce the formation of sodium adduct peaks by adding AP as additive to the ILMs. For this purpose TMG-CHCA, DIEA-CHCA, TMG-THAP, BuA-THAP, HxA-THAP, DIEA-THAP, BuA-DHB and HxA-DHB matrices were tested adding di-ammonium hydrogen phosphate (AP) in concentrations of 2.5 mM and 25 mM, respectively. The effect of the additive on the spectrum quality and the detectable number of glycopeptides is specified for each ILM in Table 3.3. In Fig 3.7 the improvements in spectra quality are illustrated by showing the best spectra that could be gained for each ILM.



**Table 3.3:** Effect of AP concentration in ILMs on the spectrum quality tested for two concentrations in the positive as well as in the negative ionization mode. The numbers specify the glycopeptides detected in the tryptic AGP-digest. + stands for improved spectrum; ++ for significantly improved spectrum; - for decreased spectrum in comparison to the ILM spectrum obtained without adding AP.

ILM	ILM-quantity per spot	positive ion mode		negative ion mode		detected glycopeptides	
		2.5 mM AP	25 mM AP	2.5 mM AP	25 mM AP	pos. ion mode	neg. ion mode
TGM-CHCA	200 µg	-	-	+	+	0	5
DIEA-CHCA	200 µg	-	++	+	++	5	5
TMG-THAP	150 µg	++	++	++	++	5	5
BuA-THAP	150 µg	+	-	++	-	5	5
HxA-THAP	150 µg	-	-	-	+	3	3
DIEA-THAP	150 µg	-	+	++	++	2	0
BuA-DHB	200 µg	no effect	-	no effect	-	5	1-3
HxA-DHB	200 µg	-	-	-	-	5	1-3

With the tryptic digest of bovine AGP as test-sample, best results were achieved applying DIEA-CHCA, TMG-THAP and BuA-THAP. With these ILMs the formation of sodium adduct peaks was reduced upon the addition of AP when working in the positive ionization mode and was nearly completely suppressed when measuring in the negative mode leading to enhanced sensitivity and S/N ratio. This effect is illustrated in the Figs. 3.5 and 3.6 comparing exemplary spectra obtained with DIEA-CHCA with and without AP. When using DIEA-CHCA, TMG-THAP and BuA-THAP two additional tryptic glycopeptides not detected with the conventional solid matrix THAP could be found with high signal intensities in the positive as well as in the negative ionization mode. It was found that BuA-THAP required an increased concentration of AP in comparison to DIEA-CHCA and TMG-THAP.

When applying TGM-CHCA the formation of multiple sodium adduct could be avoided by the addition of AP in the negative ionization mode, and all five tryptic glycopeptides were found though their intensities were very low. In the positive

ionization mode no analyte signals were observable due to the enhanced noise in the spectrum.

When using HxA-THAP in combination with AP the same three glycopeptides also detected with the conventional solid matrix THAP could be found with low signal intensities in the positive as well as in the negative ionization mode. Additionally to this finding by adding AP at a concentration of 25 mM the sodium adduct formation was reduced in negative but not in the positive mode in comparison to the spectra obtained without adding AP.

The presence of multiple sodium adduct peaks could be avoided applying DIEA-THAP in combination with AP in both ionization modes, but unfortunately only the two bigger glycopeptides within the test-sample could be observed in the positive and none at all in the negative mode. Furthermore some additional peaks were found

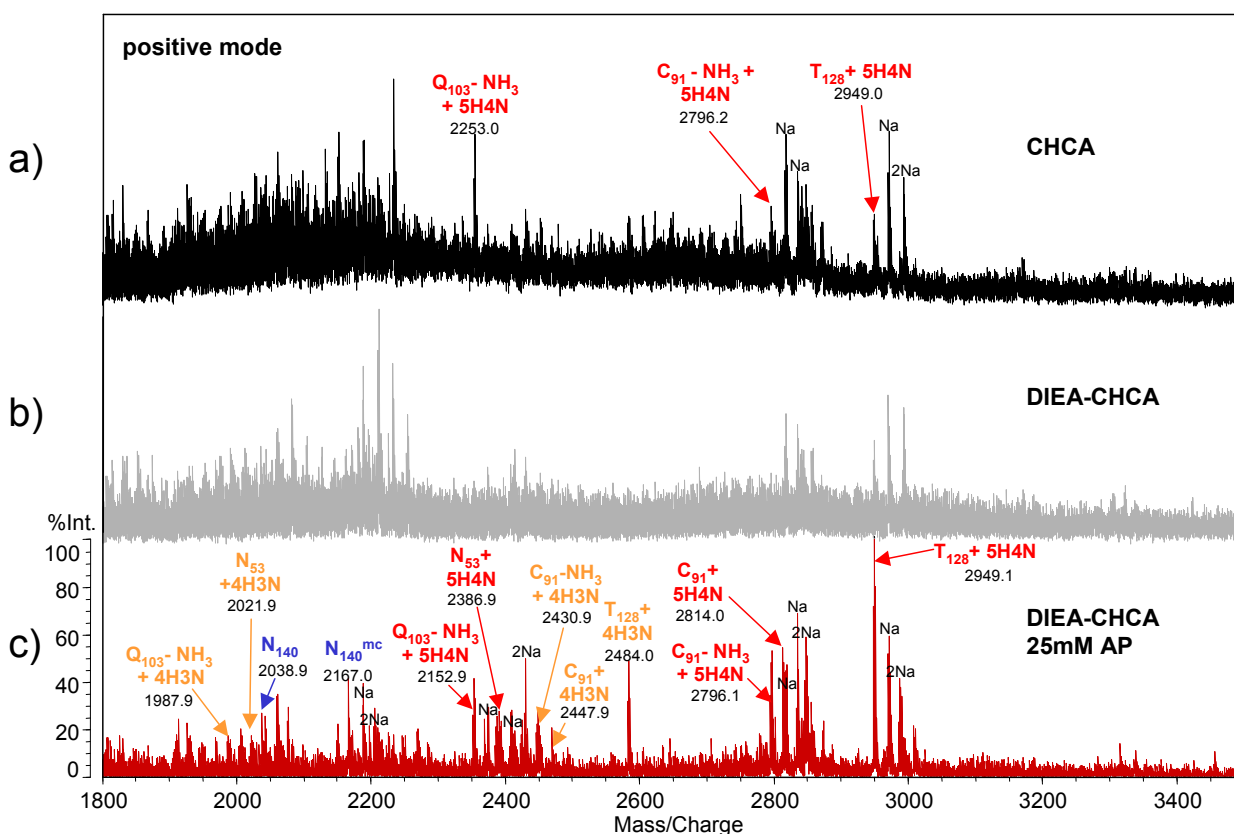


**Figure 3.5:** MALDI-QIT-rTOF mass spectra of an unseparated tryptic digest of bovine AGP in the positive ion mode obtained by using (a) CHCA as solid matrix; (b) DIEA-CHCA as ILM (without adding AP); and (c) DIEA-CHCA as ILM adding AP to a final concentration of 25 mM AP. Numerical values specify the monoisotopic masses of the  $[M+H]^+$  ions; n Na indicates the ion  $[M-(n-1)H+nNa]^+$ . H stands for Hex; N for GlcNAc; other abbr. as specified in Fig. 3.1.

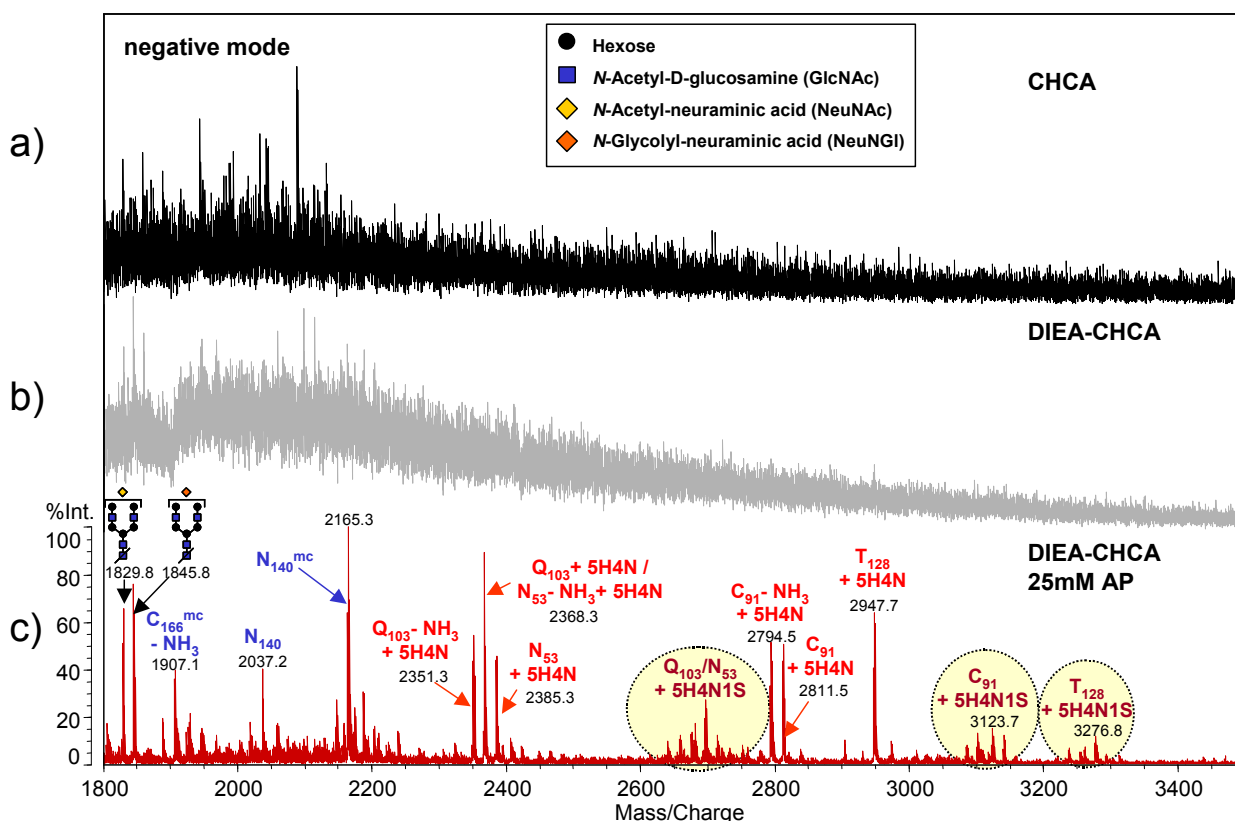


**Figure 3.6:** MALDI-QIT-rTOF mass spectra of an unseparated tryptic digest of bovine AGP in the negative ion mode obtained by using (a) CHCA as solid matrix; (b) DIEA-CHCA as ILM (without adding AP); and (c) DIEA-CHCA as ILM adding AP to a final concentration of 25 mM AP. Numerical values specify the monoisotopic masses of the  $[M-H]^-$  ions; n Na indicates the ion  $[M-(n+1)H+nNa]^-$ . S stands for SAs (*N*-acetyl-neuraminic acid (NeuNAc) and *N*-glycolyl-neuraminic acid (NeuNGI), respectively); H for Hex; N for GlcNAc; other abbr. as specified in Fig. 3.1.

in the spectra which could not be assigned to any compounds of the tryptic digest.

Interestingly, with the two DHB based ILMs no improvement in spectra quality could be achieved upon addition of AP, sodium adduct formation was not influenced but the S/N ratio was mostly decreased. Although all five glycopeptides present in the tryptic mixture were detectable with these ILMs in the positive ionization mode, the enhanced formation of multiple sodium adducts splits the signal intensities of the analytes into several peaks complicating thereby the spectra.

In summary, the attempt to reduce the formation of sodium adduct peaks and thereby optimize the quality of the spectra by adding complexing additives was successful with all mentioned ILMs, at least to some extent, except with those containing DHB.

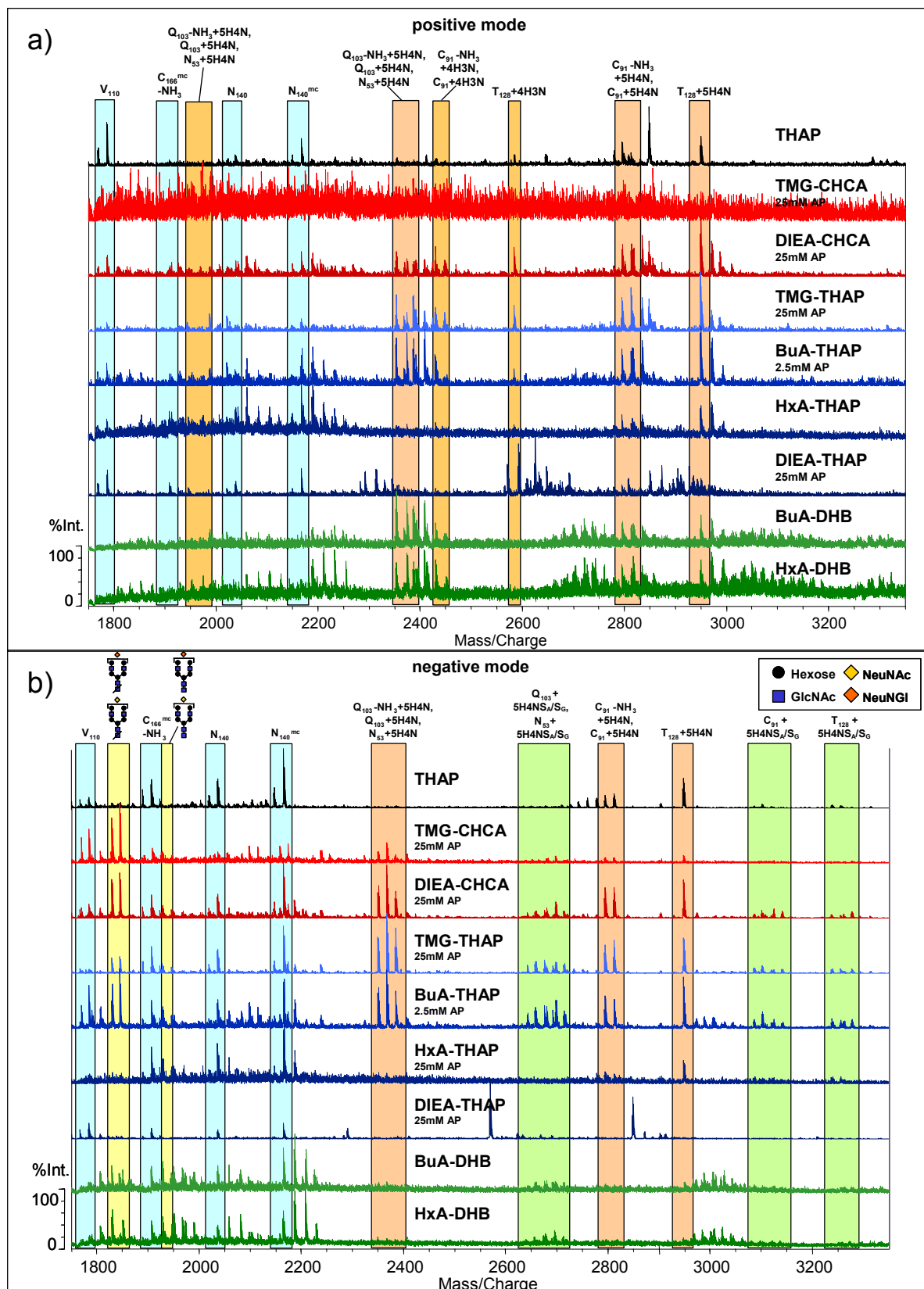


**Figure 3.7:** Best mass spectra of an unseparated tryptic AGP-digest obtainable by using ILMs in the (a) positive; and (b) negative ion mode in comparison to the solid THAP. H stands for Hex; N for HexNAc;  $S_A$  for NeuNAc;  $S_G$  for NeuNGI; other abbr. as specified in Fig. 3.1.

Regarding the detection of glycopeptides present in a complex peptide mixture best results were obtained when using DIEA-CHCA, TMG-THAP and BuA-THAP in combination with AP. Therefore, these ILMs were selected for all further investigations.

### 3.3. Ion suppression effects with ILMs

#### 3.3.1. Glycopeptides in peptide mixture

Ion suppression effects are commonly observed when dealing with glycopeptides exhibiting a rather short peptide backbone and rather large carbohydrate moieties when ionized in the presence of non-glycosylated peptides. In the case of the AGP tryptic digest investigated here as test-sample, the three glycopeptides with larger backbone could be ionized with high intensities when using THAP as solid matrix, whereas the two glycopeptides with only six and seven amino acids in the peptide backbone were not efficiently ionized. Consequently, these two glycopeptides do

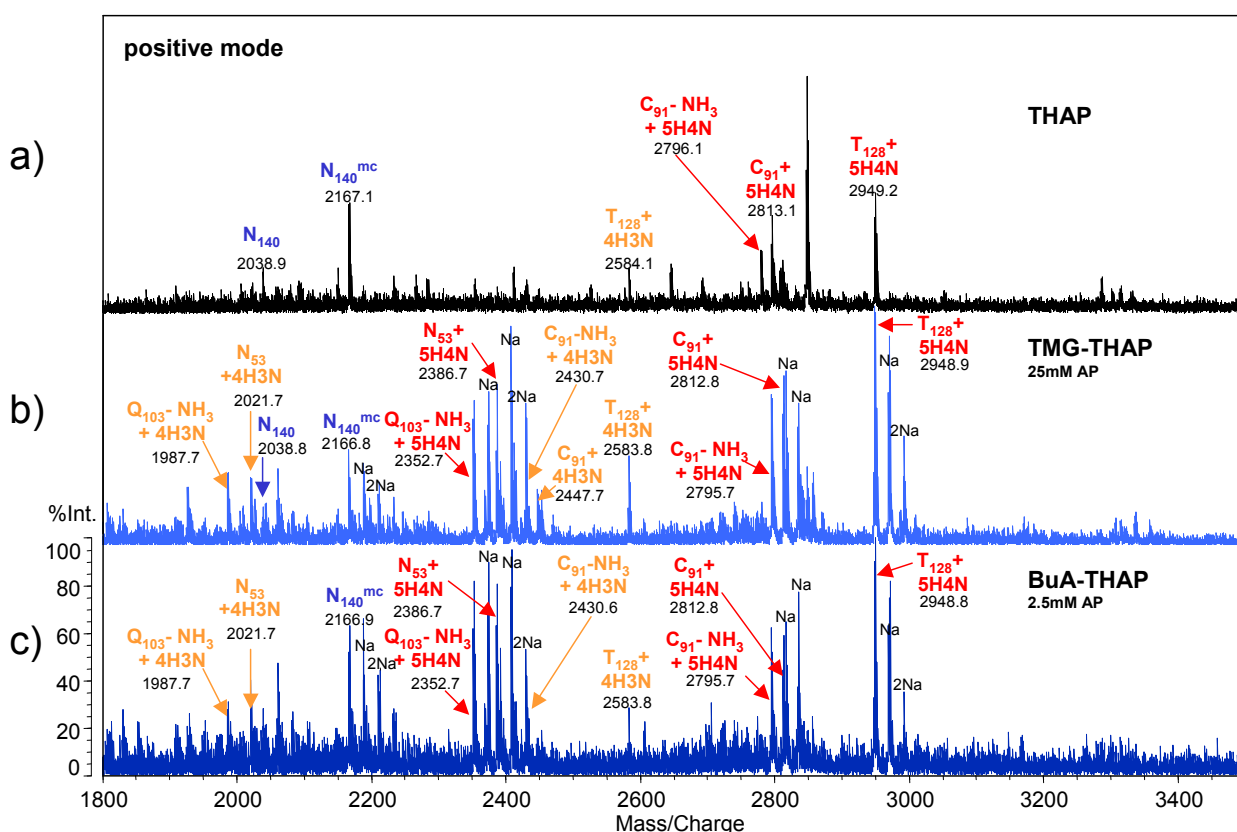


**Figure 3.8:** MALDI-QIT-rTOF mass spectra of an unseparated tryptic digest of bovine AGP in the positive ion mode obtained by using (a) THAP as solid matrix; (b) TGM-THAP as ILM (adding AP to a final conc. of 25 mM AP); and (c) BuA-THAP as ILM (adding AP to a final conc. of 2.5 mM AP). Numerical values specify the monoisotopic masses of the  $[M+H]^+$  ions; n Na indicates the ion  $[M-(n-1)H+nNa]^+$ . Abbr. as specified in Fig. 3.1.

not appear in the spectrum, neither in the positive (Fig. 3.8a) ionization mode, nor in the negative (Fig. 3.9a) mode. In contrast to this finding, when using ILMs (TMG-THAP, BuA-THAP and DIEA-CHCA) all five biantennary glycoforms could be detected in the unseparated tryptic digest, in the positive (Fig. 3.8b,c, Fig. 3.5c) as well as in the negative ionization mode (Fig. 3.9b,c, Fig. 3.6c). The very low abundant peptides with triantennary glycoforms could not be found due to the enhanced noise of the spectrum.

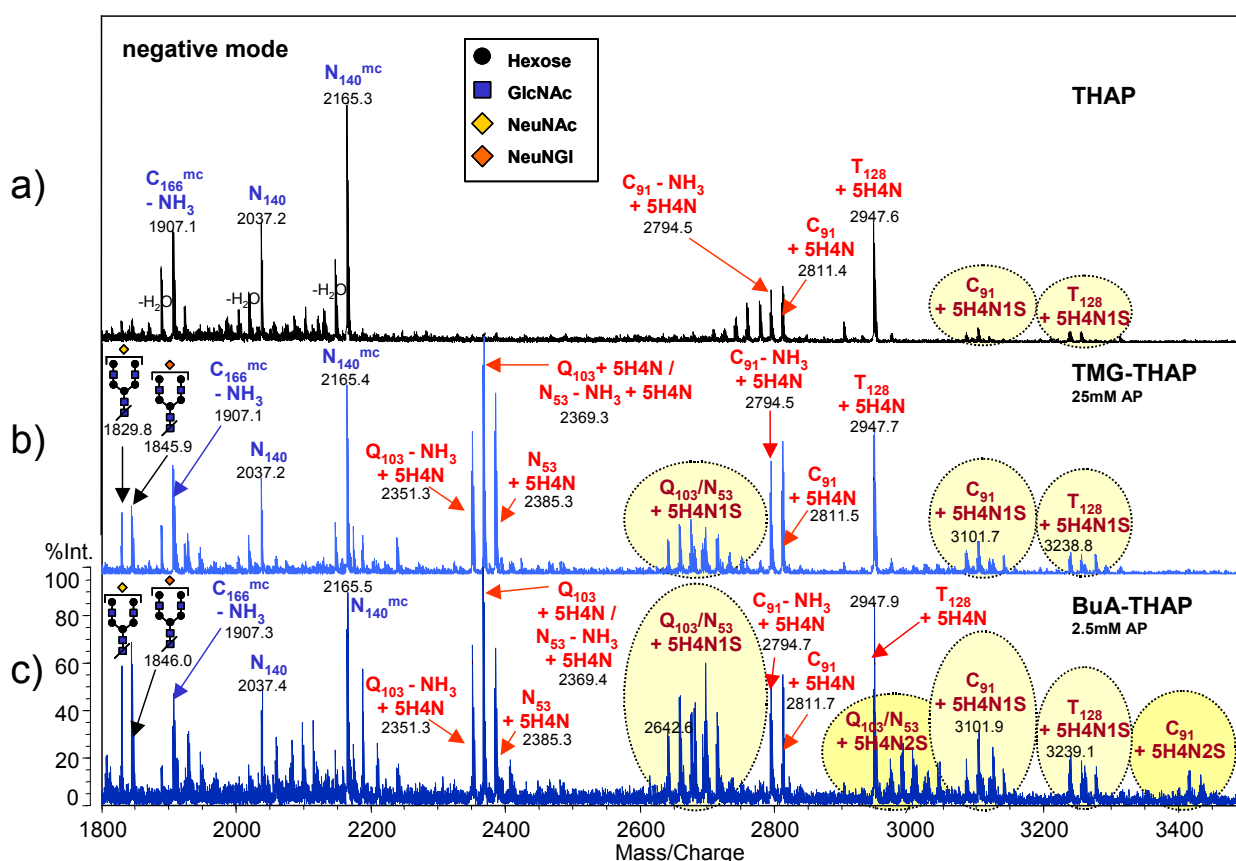


**Figure 3.9:** MALDI-QIT-rTOF mass spectra of an unseparated tryptic digest of bovine AGP in the negative ion mode obtained by using (a) THAP as solid matrix; (b) TGM-THAP as ILM (adding AP to a final conc. of 25 mM AP); and (c) BuA-THAP as ILM (adding AP to a final conc. of 2.5 mM AP). Numerical values specify the monoisotopic masses of the  $[M-H]^-$  ions. S stands for SAs (NeuNAc and NeuNGI); other abbr. as specified in Fig. 3.1.

### 3.3.2. Cleaved glycans in peptide mixture

For analyzing glycans cleft from the glycopeptides by treatment with endoglycosidases, e.g. PNGase F, a sufficient ionization yield for the glycan in presence of the tryptic peptides is required. When analyzing the mixture of glycans and tryptic peptides of bovine AGP in the positive ion mode by using THAP as solid matrix, the predominant glycan (biantennary without the terminal *N*-acetyl- and *N*-glycolyl-neuraminic acids) could be found as sodium adduct and to a very small extent only, if at all (Fig. 3.10a). Protonated ions of the glycan were not detected. The corresponding analysis in the negative ion mode gave a singly deprotonated glycan ion, this time with one SA still attached, but again with very low signal intensity (Fig. 3.14a). Using the solid matrix, the signals of oligosaccharides were nearly completely suppressed in the presence of peptides.

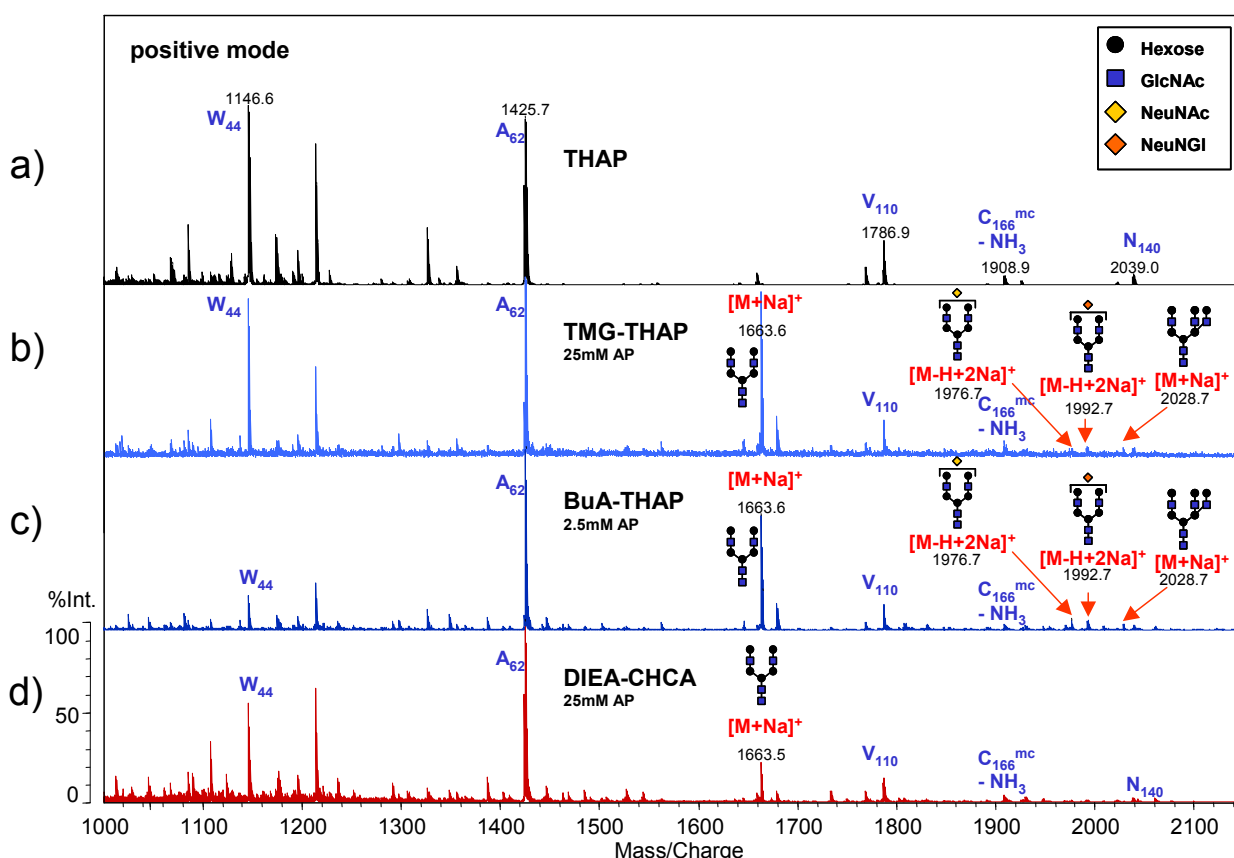


**Figure 3.10:** MALDI-QIT-rTOF mass spectra of a tryptic digest of bovine AGP after PNGase F treatment. Experimental conditions: positive ion mode, Mid 750+ Da mass range; (a) THAP as solid matrix; (b) TGM-THAP as ILM; (c) BuA-THAP as ILM; and (d) DIEA-CHCA as ILM. Numerical values specify the monoisotopic masses of the  $[M+H]^+$  ions, if not indicated otherwise. Abbr. as specified in Fig. 3.1.



When using the ILMs TMG-THAP, BuA-THAP and DIEA-CHCA the results of the corresponding measurements were quite different. Very intense signals of the biantennary glycan (without and with one SA) were observed in the positive ion mode (Fig. 3.10b,c,d) and even the minor abundant triantennary glycans could be detected when using TMG-THAP (Fig. 3.10b, Fig. 3.11b) and BuA-THAP (Fig. 3.10c), all of them as sodium adducts. The identity of the triantennary glycan structure was confirmed by the CID spectra measured in the MS<sup>2</sup> mode (Fig. 3.12).

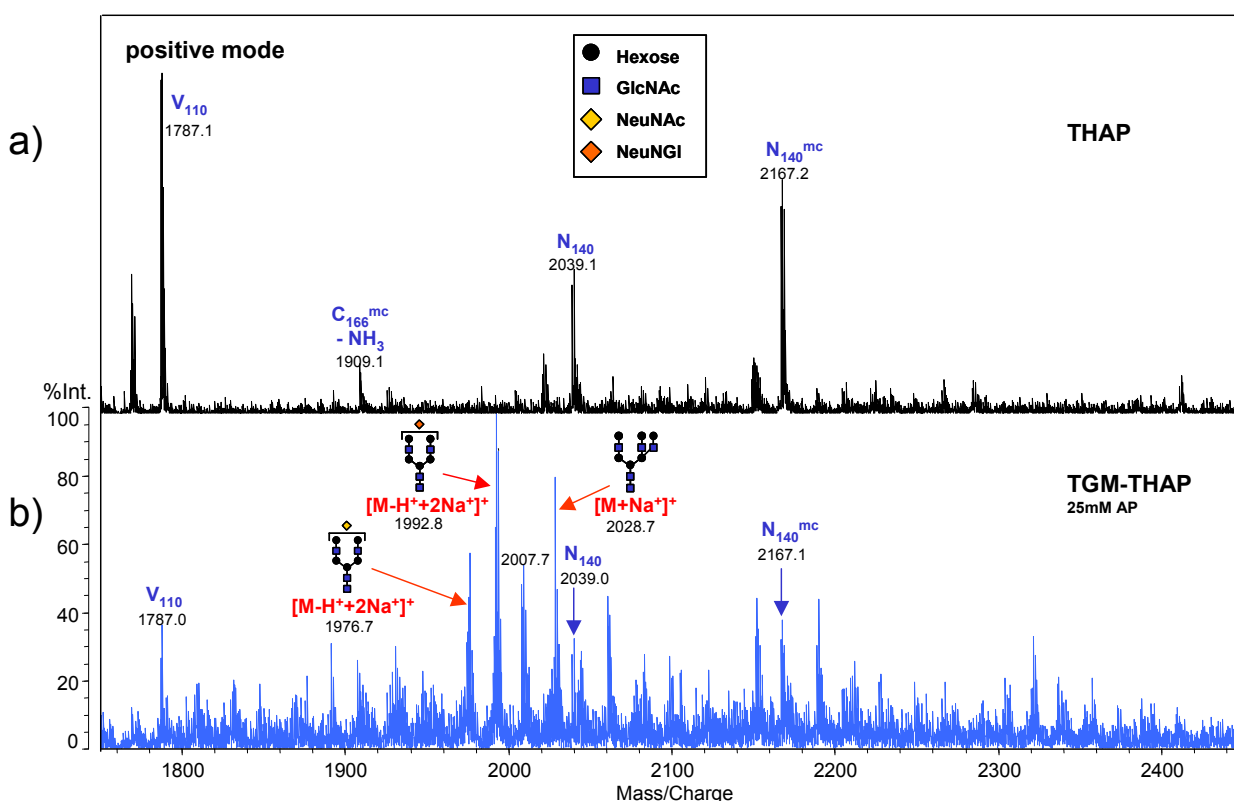


**Figure 3.11:** MALDI-QIT-rTOF mass spectra of a total tryptic digest of bovine AGP after PNGase F treatment. Experimental conditions: positive ion mode, High 2000+ Da mass range; (a) THAP as solid matrix; and (b) TGM-THAP as ILM. Numerical values specify the monoisotopic masses of the  $[M+H]^+$  ions, if not indicated otherwise.

The corresponding analysis carried out in the negative ion mode did not show the peaks of the triantennary glycan although the biantennary glycoforms are represented with high signal intensities (Fig. 3.13b,c,d). Glycans were present as deprotonated ions with one SA, as the corresponding  $^{0,2}A_7$ -cross ring fragments and also the deprotonated sodium adduct ions containing two SAs as well as

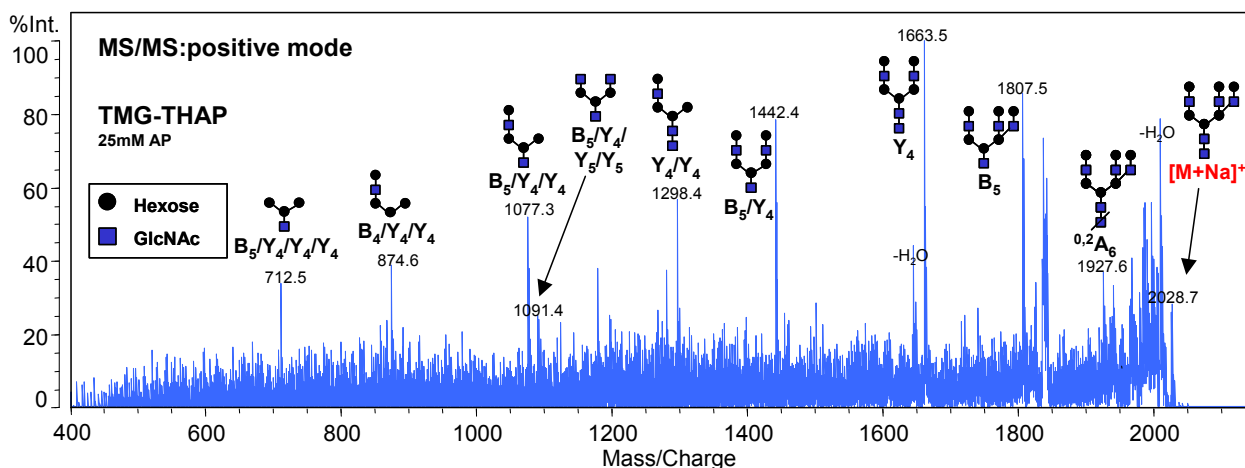


**Figure 3.12:** MS<sup>2</sup> spectrum of a triantennary complex glycan of bovine AGP taken from the unseparated tryptic digest after PNGase F treatment and using TMG-THAP as ILM. Experimental conditions: positive ion mode; precursor ion:  $m/z = 2028.7$ , corresponding to the sodiated glycan without terminal SAs. Monoisotopic masses of the  $[M+Na]^+$  ions. For nomenclature of fragment ions see Figure 3.16.

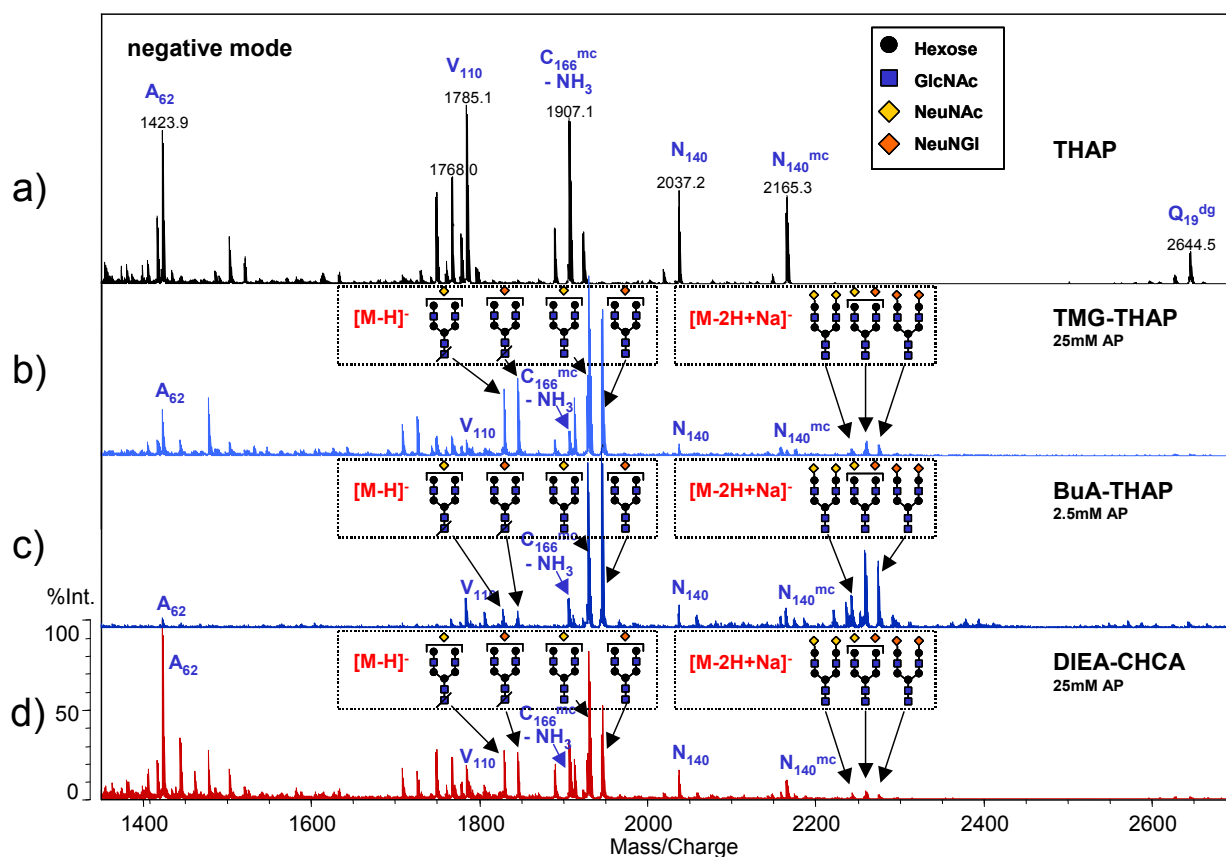


**Figure 3.13:** Mass spectra of a tryptic digest of bovine AGP treated with PNGase F. Experimental conditions: negative ion mode, Mid 750+ Da mass range; (a) THAP as solid matrix; (b) TGM-THAP as ILM; (c) BuA-THAP as ILM; and (d) DIEA-CHCA as ILM. Monoisotopic masses of the  $[M-H]^-$  ions, if not indicated otherwise; dg stands for a deglycosylated peptide.

$^{0,2}A_7$ -cross ring fragments. (For nomenclature of fragment ions see Figure 3.16.)

The Figs. 3.11 and. 3.14 demonstrate that the ionization yield of glycans in a mixture with peptides could not only be increased significantly by using the ILMs TMG-THAP, BuA-THAP and DIEA-CHCA, moreover non-glycosylated peptides were suppressed and carbohydrate structures were favored in the MALDI process. On this basis, it might be possible to confirm the presence or absence of glycans in a mixture simply by comparing the spectra obtained by using the ILMs and THAP, respectively.

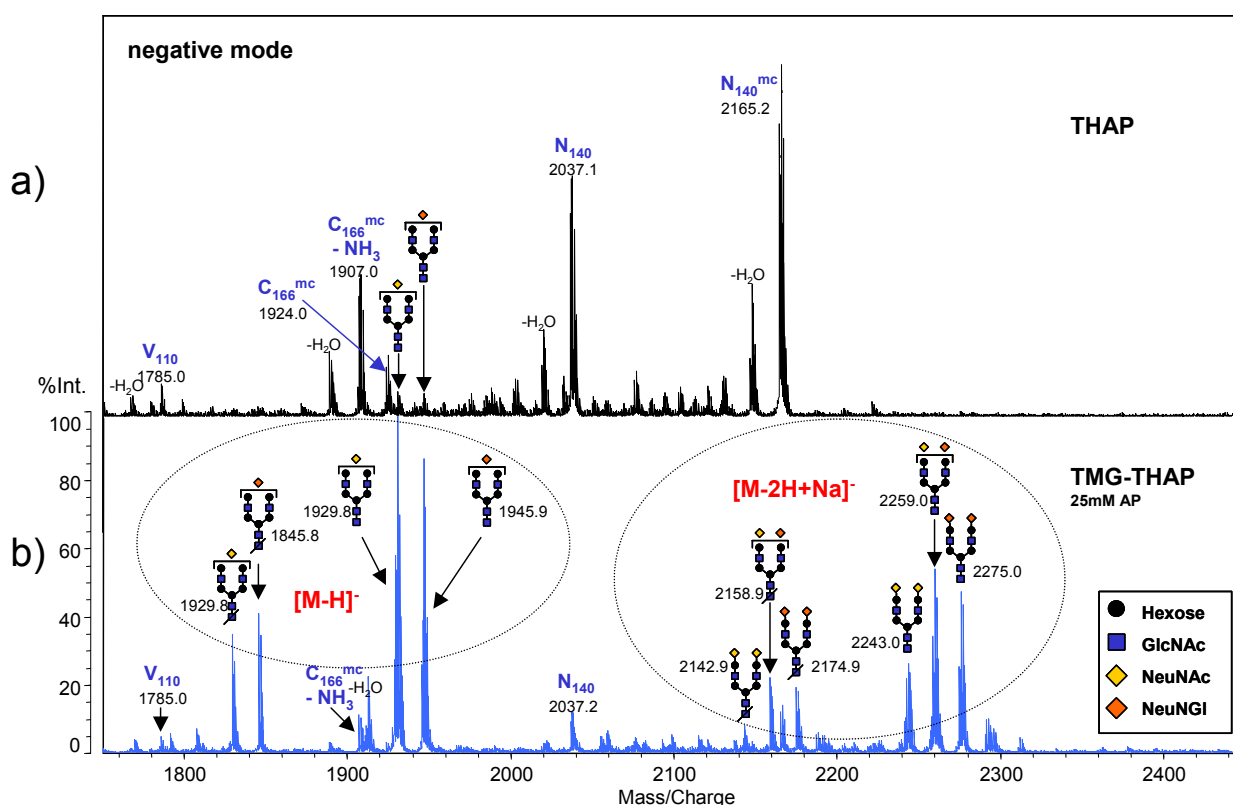


**Figure 3.14:** Mass spectra of a tryptic digest of bovine AGP after PNGase F treatment. Experimental conditions: negative ion mode, High 2000+ Da mass range; (a) THAP as solid matrix; (b) TGM-THAP as ILM; monoisotopic masses of the  $[M-H]^-$  ions, if not indicated otherwise.

### **3.4. Reduction of in-source and post-source decay by means of ILMs**

Using MALDI-MS, ISD and PSD of labile structures is commonly taking place. Whereas ISD can be observed even with linear TOF analyzers, PSD fragmentation is observed only when using rTOF or TOF-TOF or QIT-TOF instrumentation.

With the used MALDI-QIT-rTOF instrument the residence times of ions in the ion trap are in the order of milliseconds and collision events with He atoms aimed for ion-cooling take place. With this instrument a certain extent of fragmentation of labile structures is thus observed even when working in the MS<sup>1</sup> mode without intended ion fragmentation. The investigations here address the question whether or not the use of ILMs can reduce the extent of ISD and PSD of glycan structures. Such a reduction of ISD was impressively observed when investigating linear pullulans in the molecular mass range of above 5.000 [33].

#### **3.4.1. Sialylated glycopeptides in peptide mixture**

When using the described MALDI-QIT-rTOF instrument, all glycopeptides of the tryptic digest of AGP were detected as ions in which terminal SAs (*N*-acetyl- and *N*-glycolyl-neuraminic acids) were cleft off. When using the positive ionization mode, the loss of this moiety was more or less complete and was observed with all types of matrices, solid (THAP) as well as ILMs (TMG-THAP, BuA-THAP and DIEA-CHCA) (Fig. 3.8, Fig. 3.5) and were observed for the  $[M+H]^+$  as well as the  $[M+Na]^+$  and  $[M-H+2Na]^+$  ions. Beyond the cleavage of the terminal SAs, also the loss of one hexose (Hex) plus one *N*-acetyl-D-glucosamine (GlcNAc) was observed to a small extent with all glycopeptides and with all types of matrices.

When using the negative ionization mode in combination with all types of matrices the cleavage of the SAs from the glycopeptides was not complete and corresponding ions with one SA (Fig. 3.9a,c, Fig. 3.6c) were detected, and when using BuA-THAP as ILM also the ions with two SAs (Fig. 3.8b).

Although the degree of these fragmentations was reduced to some extent when using the ILMs (TMG-THAP, BuA-THAP and DIEA-CHCA), it is still high. Moreover,

in the negative ionization mode (only detectable when using ILMs) cross ring-fragmentations, particularly of the  $^{0,2}A$ -type, become significant. This is illustrated by the rather intense peak of the  $^{0,2}A_7$ -cross ring fragments at  $m/z = 1829.7$  and  $m/z = 1847.7$ , respectively, corresponding to the deprotonated biantennary glycans with one SA (*N*-acetyl- and *N*-glycolyl-neuraminic acid, respectively).

### 3.4.2. Sialylated glycans in peptide mixture

When analyzing the glycans cleft off from the tryptic peptides by PNGase F treatment by using the ILMs (TMG-THAP, BuA-THAP and DIEA-CHCA) in the positive ion mode the sodium adduct ion of the biantennary glycan having lost both terminal SAs was observed with high signal intensity (Fig. 3.10b,c,d). Ions containing one SA, either *N*-acetyl-neuraminic acid (NeuNAc) or *N*-glycolyl-neuraminic acid (NeuNGI), were present to a small extent only as di-sodiated ions ( $[5H4N1S_A-H+2Na]^+$ ,  $[5H4N1S_G-H+2Na]^+$ ). The minor abundant triantennary glycans were found as sodium adduct without the terminal SAs using TMG-THAP (Fig. 3.10b, Fig. 3.11b) and BuA-THAP (Fig. 3.10c) as ILM.

Again, in the negative ion spectra biantennary glycoforms with one SA ( $[5H4N1S_A-H]^-$  and  $[5H4N1S_G-H]^-$ ), and to a smaller extent also with two SAs ( $[5H4N2S_A-2H+Na]^-$ ,  $[5H4N1S_A1S_G-2H+Na]^-$ ,  $[5H4N2S_G-2H+Na]^-$ ) as well as their  $^{0,2}A_7$ -cross ring fragments are present (Fig. 3.13b,c,d). Glycans having lost all terminal SAs were not found at all.

Although the dissociation of the SA moieties was not completely prevented by using the ILMs, ions of the original and intact glycan such as  $[5H4N2S_A-2H+Na]^-$ ,  $[5H4N1S_A1S_G-2H+Na]^-$  and  $[5H4N2S_G-2H+Na]^-$  were detected when using the negative ion mode (Fig. 3.14a).

Other post source fragmentations like the loss of  $H_2O$  or  $NH_3$  from the peptides were found to similar extents in solid and ionic liquid matrices, respectively.

### **3.5. Enhancement of sensitivity and signal-to-noise ratio by means of ILMs**

A key aspect for or against the application of a particular MALDI-matrix is the sensitivity attainable for a certain type of sample. Therefore, sensitivities attainable with the ILMs TMG-THAP, BuA-THAP and DIEA-CHCA were compared with those attained by the solid matrix THAP. Sensitivity of detection and noise level determine together the LOD attainable by a method.

#### **3.5.1. Sensitivities of ILMs for peptides, glycopeptides and glycans in peptide mixture in comparison to the solid matrix THAP**

The LOD attained with the ILMs (TMG-THAP, BuA-THAP and DIEA-CHCA) for peptides, glycopeptides and cleaved glycans, respectively, in a peptide mixture and measured in both, positive and negative ionization mode, are listed in Table 3.4.

##### **Positive ionization mode**

When dealing with glycopeptides, the LODs attainable with TGM-THAP and DIEA-CHCA were found in the low picomole range and thus being about 20 to 60 times higher compared to those found for the solid matrix THAP. Interestingly, the LOD achieved with BuA-THAP was in the high femtomole range and thus comparable to the values of the solid matrix.

When analyzing glycans present in the tryptic digest after PNGase F treatment, the LODs attained with the ILMs were near 1 pmol and thus at least by a factor of 100 lower than observed with the solid matrix.

##### **Negative ionization mode**

In the negative ionization mode the results obtained with all three ILMs were quite similar being in the low picomole range. This is by a factor of 10 to 15 worse compared to the solid matrix THAP when dealing with glycopeptides and peptides, but by a factor of 100-200 better when dealing with cleaved glycans.

As an over-all result one can conclude that the use of ILMs leads to strongly improved LODs in the case of neat glycans (in the low picomole range) and worse

LODs (being also in the low picomole range) in the case of glycopeptides when being compared to a solid matrix. In all instances the analytes were ionized directly out of a tryptic peptide mixture without any pre-separation step.

**Table 3.4:** LOD attained for peptides, glycopeptides and cleaved glycans, respectively, when ionized out of a peptide mixture after tryptic digestion of bovine AGP and PNGase F treatment, respectively. (GPs stands for glycopeptides.)

	LOD: positive ion mode [pmol]				LOD: negative ion mode [pmol]			
<b>MALDI-Matrix</b>	peptides	large GPs	small GPs	glycans	peptides	large GPs	small GPs	glycans
<b>THAP</b>	0.3	0.2	0.3	100	0.3	0.2	0.3	200
<b>TMG-THAP</b> 25mM AP	1	10	15	1	5	5	5	1
<b>BuA-THAP</b> 2.5mM AP	0.3	0.8	0.8	0.2	5	5	3	1
<b>DIEA-CHCA</b> 25mM AP	0.5	10	20	1	3	3	3	2

### 3.5.2. Sequence coverage achieved using ILMs

The achievement of high sequence coverage indicates that ionization suppression effects between peptides present in a peptide mixture are rather low. Switching from the solid matrices CHCA and THAP, respectively, to the ILMs resulted in all cases in an improvement of sequence coverage from 69 % (CHCA) and 86 % (THAP) to about 96 %, measured for the tryptic digest of bovine AGP (see Table 3.5).

There are two main reasons for the improvement of the sequence coverage: First, the improved ionization yield of glycopeptides with small peptide backbones, and second, the absence of interfering peaks generated by conventional solid matrices like THAP or CHCA which facilitates the detection of tryptic peptides in the low-mass region. This is illustrated by the spectra in Fig. 3.15. The peptides detected by use of different matrices are shown in Fig. 3.16.

It is not completely clear, whether or not there is a third effect, i.e., a decrease in ionization suppression within the same type of analytes (all peptides). Such an effect

would indicate an influence of the liquid matrix itself which cannot primarily be explained by the predominance of different types of ions (protonated vs. sodiated) when dealing with conventional solid matrices and ILMs, respectively.

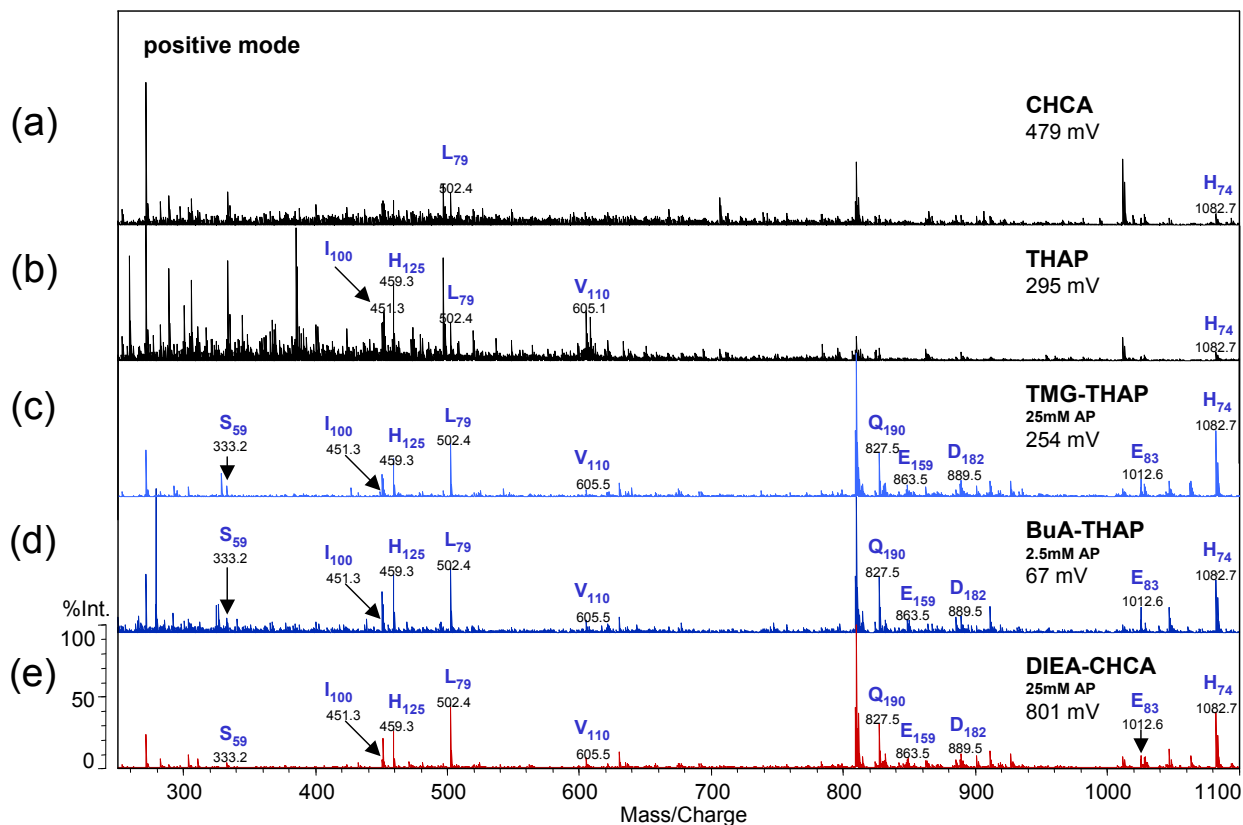


**Figure 3.15:** Mass spectra of a tryptic digest of bovine AGP: (a) CHCA and (b) THAP as solid matrices; (c) TGM-THAP and (d) BuA-THAP and (e) DIEA-CHCA as ILMs. Experimental conditions: positive ion mode; all spectra were acquired by averaging 200 unselected single laser shots. Numerical values specify the monoisotopic masses of the  $[M+H]^+$  ions. Abbr. as specified in Fig. 3.1.



THAP				
1	<i>MALLWALAVL</i>	SHLPLLD <u>QS</u>	<u>PECANLMTVA</u>	30
31	<u>PIT</u> <u>NATMDLL</u>	<u>SGK</u> <u>W</u> <u>FYIGSA</u>	<u>FRN</u> <u>PEYN</u> <u>KS</u> <u>A</u>	60
61	<u>RAIQAAFFYL</u>	<u>EPR</u> <u>HAEDK</u> <u>LI</u>	<u>TREYQTIEDK</u>	90
91	<u>CVY</u> <u>NCSFIK</u> <u>I</u>	<u>YRQ</u> <u>NG</u> <u>TL</u> <u>SKV</u>	<u>ESDREHFVDL</u>	120
121	<u>LLSK</u> <u>H</u> <u>FRTFM</u>	<u>LAASW</u> <u>NG</u> <u>TKN</u>	<u>VGVSFYADKP</u>	150
151	<u>EVTQE</u> <u>Q</u> <u>KKEF</u>	<u>LDVIK</u> <u>CIGIQ</u>	<u>ESEIIYTDEK</u>	180
181	<u>KD</u> <u>ACG</u> <u>PLEKQ</u>	<u>HEEER</u> <u>KK</u> <u>ETE</u>	<u>AS</u>	202

CHCA				
1	<i>MALLWALAVL</i>	SHLPLLD <u>QS</u>	<u>PECANLMTVA</u>	30
31	<u>PIT</u> <u>NATMDLL</u>	<u>SGK</u> <u>W</u> <u>FYIGSA</u>	<u>FRN</u> <u>PEYN</u> <u>KS</u> <u>A</u>	60
61	<u>RAIQAAFFYL</u>	<u>EPR</u> <u>HAEDK</u> <u>LI</u>	<u>TREYQTIEDK</u>	90
91	<u>CVY</u> <u>NCSFIK</u> <u>I</u>	<u>YRQ</u> <u>NG</u> <u>TL</u> <u>SKV</u>	<u>ESDREHFVDL</u>	120
121	<u>LLSK</u> <u>H</u> <u>FRTFM</u>	<u>LAASW</u> <u>NG</u> <u>TKN</u>	<u>VGVSFYADKP</u>	150
151	<u>EVTQE</u> <u>Q</u> <u>KKEF</u>	<u>LDVIK</u> <u>CIGIQ</u>	<u>ESEIIYTDEK</u>	180
181	<u>KD</u> <u>ACG</u> <u>PLEKQ</u>	<u>HEEER</u> <u>KK</u> <u>ETE</u>	<u>AS</u>	202

TMG-THAP, BuA-THAP and DIEA-CHCA				
1	<i>MALLWALAVL</i>	SHLPLLD <u>QS</u>	<u>PECANLMTVA</u>	30
31	<u>PIT</u> <u>NATMDLL</u>	<u>SGK</u> <u>W</u> <u>FYIGSA</u>	<u>FRN</u> <u>PEYN</u> <u>KS</u> <u>A</u>	60
61	<u>RAIQAAFFYL</u>	<u>EPR</u> <u>HAEDK</u> <u>LI</u>	<u>TREYQTIEDK</u>	90
91	<u>CVY</u> <u>NCSFIK</u> <u>I</u>	<u>YRQ</u> <u>NG</u> <u>TL</u> <u>SKV</u>	<u>ESDREHFVDL</u>	120
121	<u>LLSK</u> <u>H</u> <u>FRTFM</u>	<u>LAASW</u> <u>NG</u> <u>TKN</u>	<u>VGVSFYADKP</u>	150
151	<u>EVTQE</u> <u>Q</u> <u>KKEF</u>	<u>LDVIK</u> <u>CIGIQ</u>	<u>ESEIIYTDEK</u>	180
181	<u>KD</u> <u>ACG</u> <u>PLEKQ</u>	<u>HEEER</u> <u>KK</u> <u>ETE</u>	<u>AS</u>	202

**Figure 3.16:** Sequence coverage achieved using different types of matrices: Tryptic peptides are specified alternately in orange and green letters, glycopeptides in blue letters. Glycosylation sites are marked in dark blue letters. Not detected peptides and glycopeptides are highlighted in gray. The cleft signal peptide is indicated in italic.

**Table 3.5:** Sequence coverage of the tryptic peptides of bovine AGP in the positive ionization mode for different matrices

<b>MALDI-Matrix</b>	<b>Sequence coverage</b>
<b>THAP</b>	<b>86.4 %</b>
<b>CHCA</b>	<b>69.0 %</b>
<b>TMG-THAP</b>	<b>96.2 %</b>
<b>BuA-THAP</b>	<b>96.2 %</b>
<b>DIEA-CHCA</b>	<b>96.2 %</b>

### 3.6. Modification in collision-induced dissociation pattern when using ILMs

When dealing with complex mixtures of biomolecules, MALDI-MS<sup>2</sup> is often an essential requirement for identification and characterization of these biomolecules and parts thereof. This chapter addresses the question whether and how far CID pattern of glycopeptides and glycans are influenced by the type of matrix used. In this investigation low energy CID is used as it usually takes place in ion traps by collision of analyte ions with argon atoms. CID spectra obtained by using the ILM TMG-THAP were compared with those obtained by using the solid matrix THAP. All MS<sup>2</sup>-spectra were generated out of the unseparated mixtures. The nomenclature for specifying the fragment ions of the glycans is presented in Fig. 3.16 according to Domon and Costello [68].

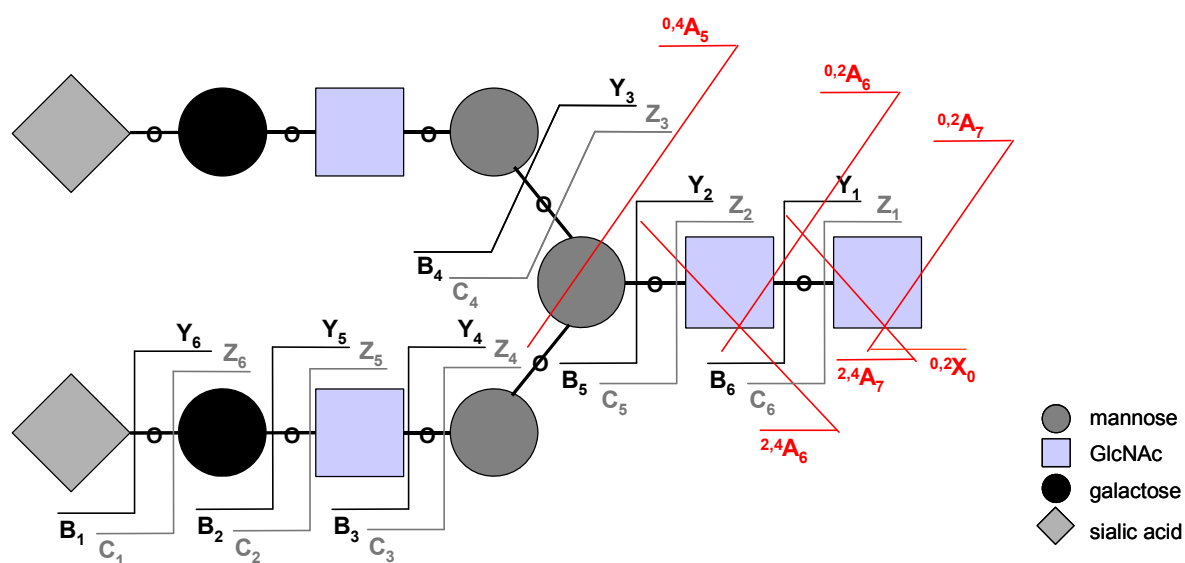


**Figure 3.16:** Simplified illustration of the nomenclature for carbohydrate fragmentation proposed by Domon and Costello [68]. A, B and C stand for fragments containing the non-reducing end of the oligosaccharide, whereas X, Y and Z represent ions still containing the reducing end of the oligosaccharide. Subscripts indicate the position relative to the termini and superscripts are used to specify the cleavage sites within sugar rings.

### 3.6.1. Glycopeptides

As an example for the CID pattern of glycopeptides in the positive ionization mode the spectra of the glycopeptide  $T_{128}$  are shown in Fig. 3.17, comparing TMG-THAP and THAP as MALDI-matrices.  $T_{128}$  carries a biantennary glycan of the complex type. Both spectra were very similar, even when considering the relative intensities of fragment ions. As known for low-energy CID of glycopeptides, there is a predominance of Y type ions resulting from cleavages of the glycosidic bonds. In addition, there is a series of peaks originating from stepwise losses of water and cross-ring fragmentations of the core-GlcNAc. These peaks are located between the signals of the neat peptide ( $m/z = 1326.8$ ) and that with one single GlcNAc ( $m/z = 1529.9$ )

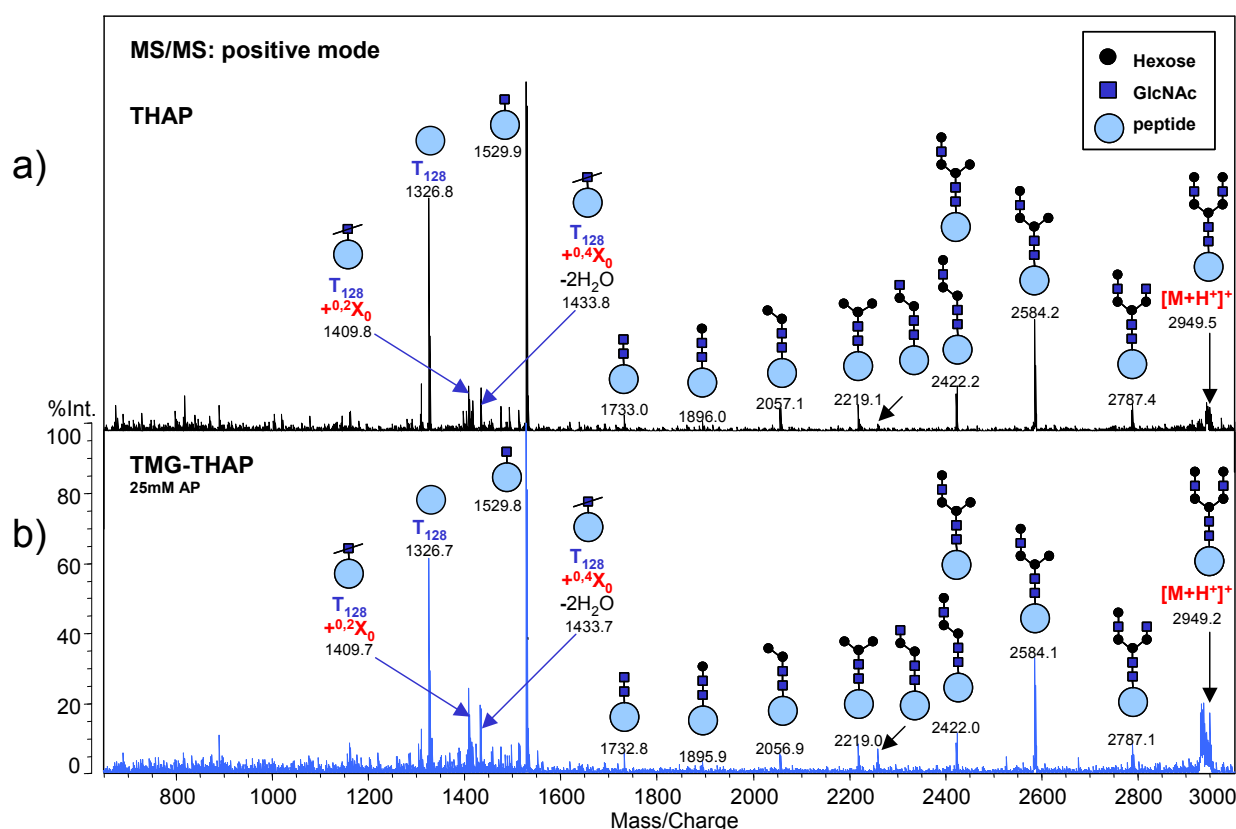


**Figure 3.17:** MS<sup>2</sup> spectrum of glycopeptide  $T_{128}$  of bovine AGP taken from the unseparated tryptic digest. Experimental conditions: positive ion mode; (a) THAP as solid matrix; and (b) TMG-THAP as ILM; precursor ion:  $m/z = 2949.2$  corresponding to the protonated peptide  $T_{128}$  carrying a N-linked biantennary complex glycan without terminal sialic acids (SAs). Numerical values specify the monoisotopic masses of the  $[M+H]^+$  ions. For nomenclature of fragment ions see Figure 3.16.

For illustration of the CID pattern of glycopeptides in the negative ionization mode the glycopeptide C<sub>91</sub> was chosen as example. This peptide again carries a biantennary complex-type glycan, and Fig. 3.18 displays the spectra of C<sub>91</sub> using THAP and TMG-THAP, respectively. Again, in both spectra the same fragment ions were formed in very similar relative intensities. But, unlike to CID in the positive ion mode no predominant cleavage of the glycosidic bonds (formation of Y ions) could be observed here. The two most abundant peaks resulted from the detachment of the more or less complete glycan residue from the peptide by cross-ring fragmentation within the first core-GlcNAc. Furthermore, D ions and their dehydrated form [D-18] were observed. These types of ions have been described by Harvey as diagnostic for the composition of the 6-antenna in complex type glycans in negative-mode ESI-MS under low-energy CID conditions [69, 70].

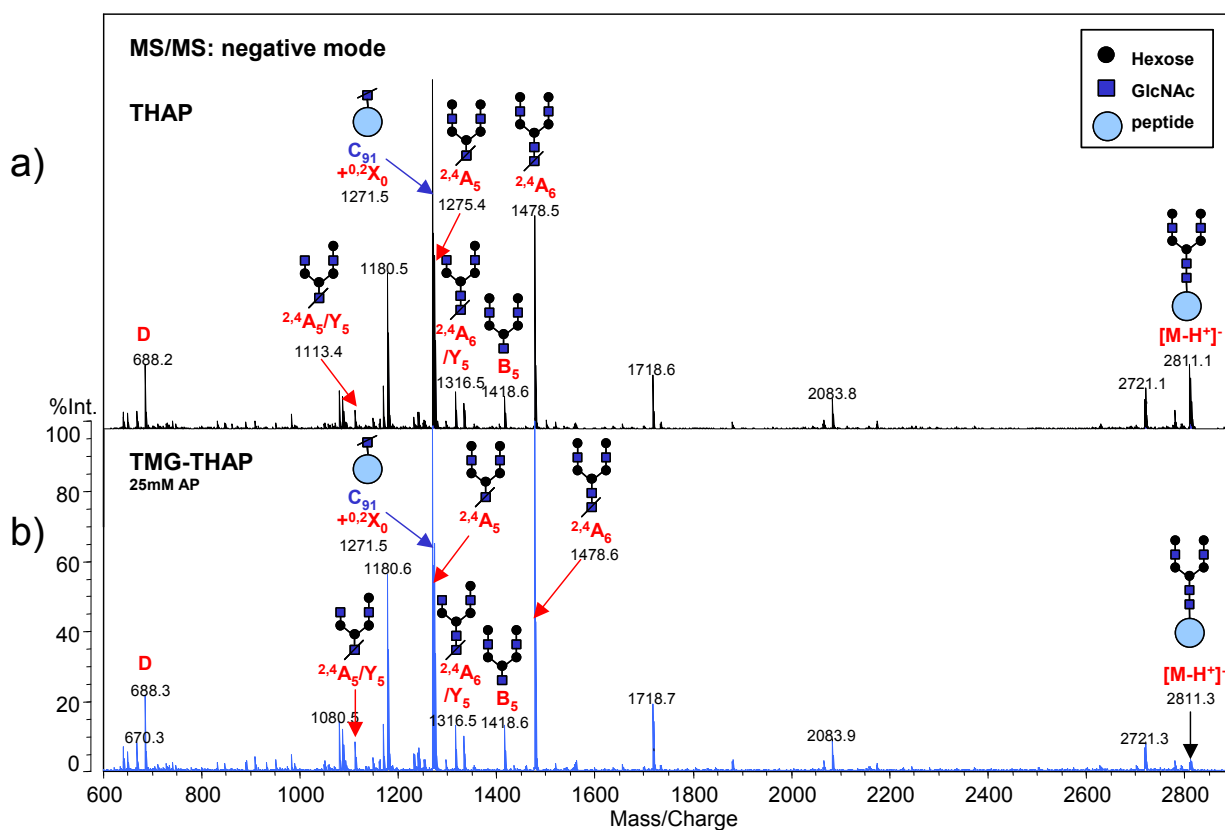


**Figure 3.18:** MS<sup>2</sup> spectrum of glycopeptide C<sub>91</sub> of bovine AGP taken from the unseparated tryptic digest. Experimental conditions: negative ion mode; (a) THAP as solid matrix; and (b) TMG-THAP as ILM; precursor ion:  $m/z = 2811.1$  corresponding to the deprotonated peptide C<sub>91</sub> carrying one *N*-linked biantennary complex glycan without terminal SAs. Numerical values specify the monoisotopic masses of the [M-H]<sup>+</sup> ions. For nomenclature of fragment ions see Figure 3.16.

### 3.6.2. Glycans

As an example for the CID pattern of glycans when using the positive ionization mode the MS<sup>2</sup> spectra of the sodiated biantennary glycan (carrying no terminal SAs) are shown in Fig. 3.19, again comparing THAP and TMG-THAP. Because of the low ionization yield for the glycan when using the solid matrix THAP, only low signal intensities could be achieved in this instance. Nevertheless, comparison of the spectra indicates that identical ions could be identified in both CID spectra. The predominant fragmentation results from cleavages of the glycosidic bonds (resulting in Y ions as well as B ions).

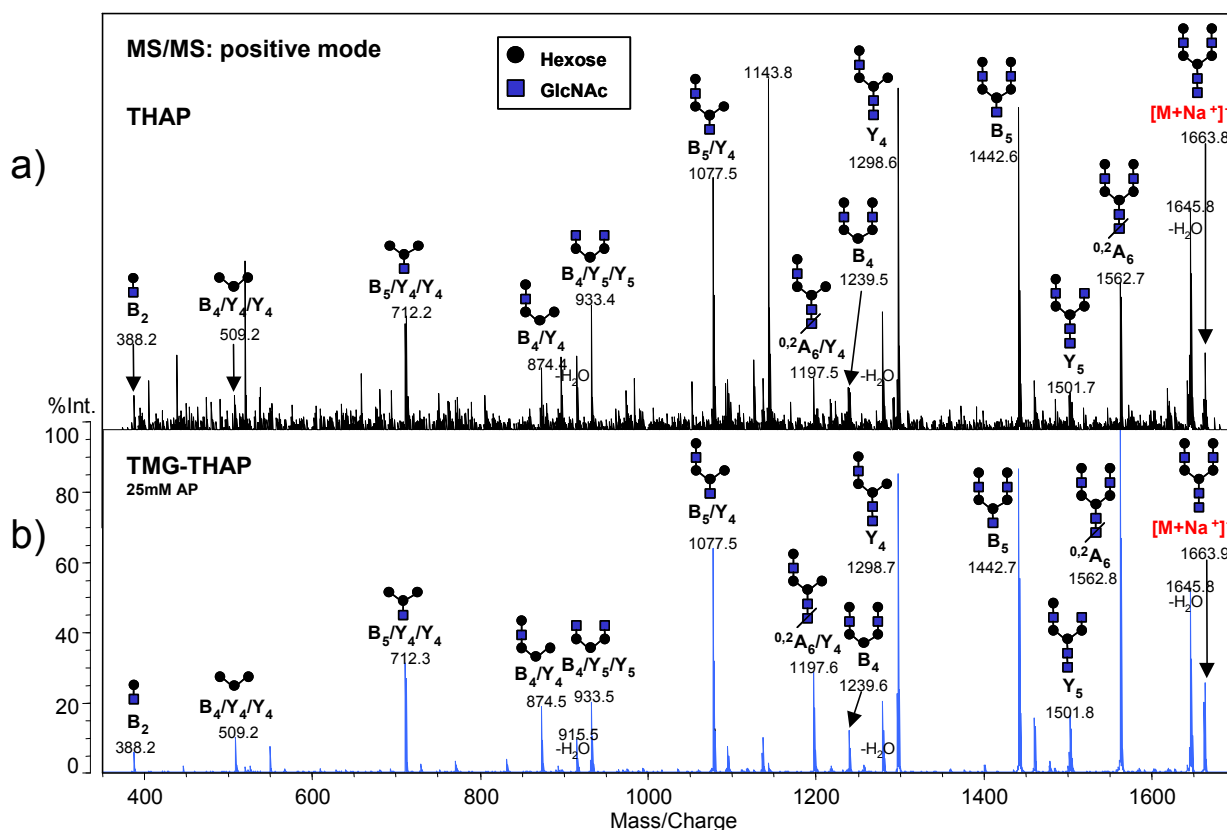


**Figure 3.19:** MS<sup>2</sup> spectrum of a biantennary complex glycan of bovine AGP taken from the unseparated tryptic digest after PNGase F treatment. Experimental conditions: positive ion mode; (a) THAP as solid matrix; and (b) TMG-THAP as ILM; precursor ion:  $m/z = 1663.9$  corresponding to the sodiated glycan without terminal SAs. Numerical values specify the monoisotopic masses of the  $[M+H]^+$  ions. For nomenclature of fragment ions see Figure 3.16.

For illustration of the CID fragmentation patterns of glycans in the negative ion mode the spectra of the monosialylated complex-type biantennary glycan with one NeuNGI are shown in Fig. 3.20. Because it is not known to which antenna the SA (probably remaining after hydrolytic cleavage of the other one) is linked, the fragment ions were numbered as if the SA was present on both antennas. Again, with both types of matrices the same ions were predominantly produced and the relative intensities were comparable. Aside from B- and Y-type ions formed by glycosidic cleavages that are common to the fragmentation of positive ions, the spectra contain abundant ions produced by cross ring cleavages of the two core-GlcNAcs.

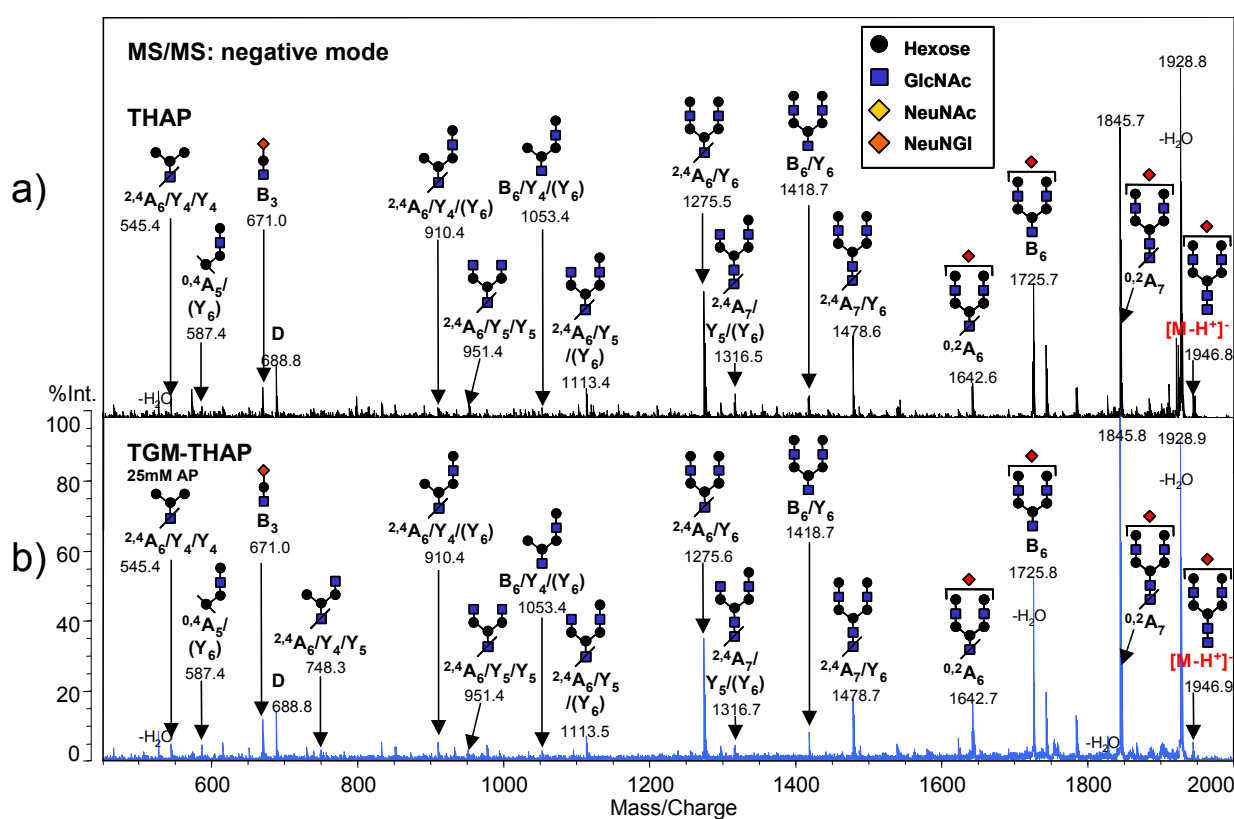


**Figure 3.20:** MS<sup>2</sup> spectrum of a complex biantennary glycan of bovine AGP with one terminal SA (in this case NeuNGI) taken from the unseparated tryptic digest after PNGase F treatment. Experimental conditions: negative ion mode; (a) THAP as solid matrix; and (b) TMG-THAP as ILM; precursor ion:  $m/z = 1946.9$ . Numerical values specify the monoisotopic masses of the  $[M-H]^-$  ions. For nomenclature of fragment ions see Figure 3.16.

In summary, when comparing the low-energy CID spectra of glycopeptides and glycans obtained with an ionic liquid matrix (TMG-THAP) and the corresponding solid matrix (THAP), no significant difference in the fragmentation pattern was observed. This is valid for the positive, as well as the negative ionization mode. The higher ionization yield attained for neat glycans in the positive mode when using the ILM resulted in much clearer MS<sup>2</sup> spectra.



### **3.7. Reproducibility of quantitative pattern using ILMs**

One of the major factors that exclude the application of MALDI-MS for quantitative analysis is the inhomogeneous segregation of the analytes in crystalline matrices. The “hot spot” formation leads to a lack of shot-to-shot and spot-to-spot reproducibility. This effect can be overcome only by working with a very high number of laser-shots and by the use of internal standards. With RTIL-preparations, within which no crystallization proceeds, the distribution of the analytes is expected to be more homogeneous and areas exhibiting different desorption characteristics (hot spots vs. spot areas giving no signals) are expected being less frequent. In ILM-preparation the reproducibility of analyte ion intensities should thus be improved.

For investigation of the spot-to-spot reproducibility in various crystalline matrices and ILMs, spectra averaged over 200 laser shots were acquired for seven different spots containing the same amount of analytes, *i.e.*, 100 pmol of bovine AGP after tryptic digestion and PNGase F treatment, respectively. Average signal intensity values (reflecting the ionization efficiency in the particular matrix) and the corresponding relative standard deviations (RSD) when measuring seven single spots each were determined for three randomly selected peptides (Table 3.6), two glycopeptides (Table 3.7) and three glycans (Table 3.8) using DIEA-CHCA, TMG-THAP and BuA-THAP as ILMs, respectively. These data were compared with the corresponding data found with the crystalline matrix THAP.

With the spot preparation procedure used here, no gain in reproducibility was found for ILMs. This finding is in some contrast to data reported previously by other groups [29, 62]. The RSD values obtained vary within a rather wide range and a general trend regarding a correlation between matrix type and reproducibility can hardly be found. It seems that RSD values obtained with DIEA-CHCA and TMG-THAP were similar or slightly higher compared to those found with THAP. With BuA-THAP the worst results were achieved. With this ILM the matrix/analyte layer did not form a planar film but contracted to small single drops or formed a ring on the target after evaporation of the solvent. Probably, in this instance an inhomogeneous segregation of the analytes within the spot area was effected. This observation indicates that

spot-to-spot reproducibility might significantly be affected by the spot size and the spot application procedure chosen.

**Table 3.6:** Spot-to-Spot reproducibility of signal intensities (mV) of three randomly selected peptides (analyzed from a peptide mixture gained by tryptic digestion of bovine AGP). Average values, standard deviation (SD) and relative standard deviation (RSD) values were assessed from seven single spots using 200 laser shots per spot.

	Positive ion mode				Negative ion mode			
Peptide	$M_r = 1146.6$				$M_r = 1144.6$			
Matrix	THAP	TGM-THAP	BuA-THAP	DIEA-CHCA	THAP	TGM-THAP	BuA-THAP	DIEA-CHCA
Average	1842	422	326	424	686	113	12	404
SD	117	171	202	151	110	42	9	119
RSD (%)	6	40	62	36	16	37	77	29
Peptide	$M_r = 1425.8$				$M_r = 1423.8$			
Matrix	THAP	TGM-THAP	BuA-THAP	DIEA-CHCA	THAP	TGM-THAP	BuA-THAP	DIEA-CHCA
Average	1539	500	742	794	435	83	24	277
SD	198	192	279	227	67	28	10	72
RSD (%)	13	39	38	29	15	33	43	26
Peptide	$M_r = 1786.9$				$M_r = 1784.9$			
Matrix	THAP	TGM-THAP	BuA-THAP	DIEA-CHCA	THAP	TGM-THAP	BuA-THAP	DIEA-CHCA
Average	293	61	84	115	412	17	47	50
SD	117	14	31	31	105	4	18	11
RSD (%)	40	22	38	27	26	23	37	23

**Table 3.7:** Spot-to-Spot reproducibility of signal intensities of two randomly selected glycopeptides (analyzed from a peptide mixture gained by tryptic digestion of bovine AGP). Average values, standard deviation (SD) and relative standard deviation (RSD) values were assessed from seven single spots using 200 laser shots per spot.

	Positive ion mode				Negative ion mode			
Glycopeptide	$M_r = 2813.2$				$M_r = 2811.1$			
Matrix	THAP	TGM-THAP	BuA-THAP	DIEA-CHCA	THAP	TGM-THAP	BuA-THAP	DIEA-CHCA
Average	41	12	17	4	70	17	24	5
SD	12.7	1.6	5.7	1.1	25.1	3.4	8.1	0.4
RSD (%)	31	13	33	28	36	20	34	8
Glycopeptide	$M_r = 2949.2$				$M_r = 2947.2$			
Matrix	THAP	TGM-THAP	BuA-THAP	DIEA-CHCA	THAP	TGM-THAP	BuA-THAP	DIEA-CHCA
Average	155	49	10	14	250	70	11	18
SD	43.5	9.3	2.2	5.1	66.9	9.4	3.8	7.7
RSD (%)	28	19	23	37	27	13	34	43

**Table 3.8:** Spot-to-Spot reproducibility of signal intensities) of three randomly selected glycans (analyzed from a peptide mixture gained by tryptic digestion of bovine AGP and PNGase F treatment). Average values, standard deviation (SD) and relative standard deviation (RSD) values were assessed from seven different spots using 200 laser shots per spot.

	Positive ion mode				Negative ion mode			
Glycan	<b>M<sub>r</sub> = 1663.6</b>				<b>M<sub>r</sub> = 1829.6</b>			
Matrix	THAP	TGM-THAP	BuA-THAP	DIEA-CHCA	THAP	TGM-THAP	BuA-THAP	DIEA-CHCA
Average	12	380	202	170	-	120	37	68
SD	4	41	95	40	-	32	37	22
RSD (%)	33	11	47	24	-	27	102	32
Glycan	<b>M<sub>r</sub> = 1992.7</b>				<b>M<sub>r</sub> = 1845.6</b>			
Matrix	THAP	TGM-THAP	BuA-THAP	DIEA-CHCA	THAP	TGM-THAP	BuA-THAP	DIEA-CHCA
Average	-	46	17	12	-	147	49	63
SD	-	11	9	4	-	35	48	23
RSD (%)	-	25	52	30	-	24	98	36
Glycan	<b>M<sub>r</sub> =2028.7</b>				<b>M<sub>r</sub> = 1946.7</b>			
Matrix	THAP	TGM-THAP	BuA-THAP	DIEA-CHCA	THAP	TGM-THAP	BuA-THAP	DIEA-CHCA
Average	-	14	11	-	-	256	294	123
SD	-	3	5	-	-	46	150	58
RSD (%)	-	23	40	-	-	18	51	47

### **3.8. Conclusions**

The aim of this work was development and optimization of ILMs for improved MALDI-MS-based analysis of glycopeptides and glycans in the presence of non-glycosylated peptides. For this purpose twelve ILs were synthesized; seven of these ILs were prepared and tested as ILM for the first time. Four of the twelve synthesized ILs formed thin solid layers on the target under room temperature conditions, the other eight ILs remained liquid at room temperature and were chosen for further investigations expecting that the liquid nature of RTILs provides certain advantages over the solid state of the commonly used crystalline matrices. After optimization of sample preparation, best results regarding the detection of glycopeptides present in a peptide mixture were obtained by the application of the ILMs DIEA-CHCA, TMG-THAP and BuA-THAP. The formation of sodium adduct peaks was reduced upon the addition of di-ammonium hydrogen phosphate (AP) when working in the positive ionization mode and was nearly completely suppressed when measuring in the negative mode leading to clearer spectra. DIEA-CHCA, TMG-THAP and BuA-THAP were demonstrated to be able to desorb/ionize the analytes with very satisfactory S/N-ratios in both, the positive and the negative ionization mode. These three ILMs were further investigated with respect to the criteria ionization efficiency and extent of fragmentation in MALDI-MS analysis of glycopeptides and glycans compared to the commonly used crystalline matrix THAP. (THAP was previously shown to give the best results when comparing the three crystalline matrices CHCA, DHB and THAP.)

The ILMs investigated, *i.e.*, DIEA-CHCA, TMG-THAP and BuA-THAP, were well suited for the analysis of glycopeptides and glycans in a mixture of peptides. When using THAP as solid matrix the two smaller glycopeptides of the test-sample (*i.e.*, the unseparated tryptic AGP-digest) were not efficiently ionized, and, thus, could not be seen in the spectrum. However, when applying the ILMs all five glycopeptides could be detected in their high abundant biantennary glycoforms in the positive ionization mode as well as in the negative one. By the use of the ILMs it was possible to overcome the ionization suppression of glycopeptides with short peptide backbones in the presence of non-glycosylated peptides.

When using the conventional matrix THAP for the analysis of a mixture of peptides and glycans (*i.e.*, unseparated tryptic AGP-digest treated with PNGase F) the signals for the cleaved oligosaccharides were nearly completely suppressed by the presence of peptides. In contrast, when measuring the identical sample with the ILMs very intense signals of the biantennary glycan were observed in both ion modes. Even the minor abundant triantennary glycans could be detected when using TMG-THAP and BuA-THAP in the positive ion mode. Moreover, it seems that the MALDI process favors glycans over peptides, mainly when measuring in the negative ionization mode. Preferential ionization of a specific analyte such as glycopeptides within a mixture could be helpful for complex samples like protein digests. E.g., the presence or absence of glycans in a mixture could simply be confirmed by comparing spectra obtained by using an ILM and THAP, respectively.

The improved ionization efficiency for carbohydrate structures (in the presence of peptides) which could be attained by the use of the three ILMs allowed the detection of glycopeptides and glycans with such high intensities that a subsequent CID-fragment analysis became feasible. Comparing the MS<sup>2</sup> spectra of glycopeptides and glycans obtained with an ionic liquid matrix (TMG-THAP) and the conventional matrix THAP, no significant difference in fragmentation pattern was observed.

Regarding the extent of cleavage of terminal SAs during the MALDI process, the following results were obtained:

Analyzing glycopeptides within the tryptic digest in the positive ionization mode, the loss of this moiety was more or less complete and was observed with all types of matrices, solid (THAP) as well as the mentioned ILMs. When measuring glycopeptides in the negative ionization mode with both types of matrices the loss of SAs was still high but species with single SAs attached were detected, when using BuA-THAP even the ions with two SAs. The extent of fragmentation could be reduced by the use of ILMs, however, it was still high.

When analyzing sialylated neat glycans in the positive ionization mode with both types of matrices ions containing one SA were present to a small extent only. Measuring in the negative mode biantennary glycoforms with one SA, and when using ILMs to a smaller extent also those with two SAs were found. Interestingly there were no glycans found which have lost all their terminal SAs. Although the loss

of the SAs was not completely avoided by the use of ILMs, intact glycan structures carrying two SAs could be detected.

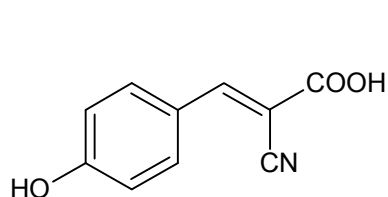
By the use of the mentioned three ILMs strongly improved LODs (in the low picomole range) in the case of cleaved glycans in the presence of peptides were achieved compared to the results attained for the solid matrix THAP (in the high picomole range). Worse LODs (being also in the low picomole range) were found in the case of glycopeptides in a peptide mixture compared to THAP (in the high femtomole range). Only the LODs obtained with BuA-THAP in positive ionization mode were comparable to those of the solid matrix.

The improved ionization yield of glycopeptides with small peptide backbones and the reduced matrix background obtained by using the mentioned ILMs resulted in an improved amino acid sequence coverage for the tryptic AGP-digest compared to the solid matrices CHCA and THAP. The absence of interfering peaks generated by conventional solid matrices allowed the detection of small tryptic peptides and might represent an advantage for the analysis of compounds in the low-mass region like amino acids or oligosaccharides.

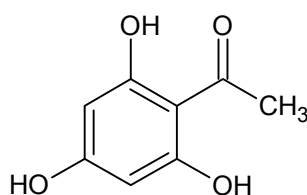
Surprisingly, the expected increase in reproducibility could not be observed. The liquid nature of the ILMs chosen should result in more homogeneous sample preparations and therefore improved spot-to-spot reproducibility. RSD values determined for peptides, glycopeptides and glycans with DIEA-CHCA and TMG-THAP were similar compared to those found with THAP. Worst results were achieved with BuA-THAP which has a tendency to form no planar spot surfaces. Therefore, further studies will be necessary addressing improvements in spot preparation. Nevertheless, ILMs did not tend to form hot-spots and therefore the number of laser shots could be reduced in comparison to classical crystalline matrices and this fact led to decreased measurement time.

## 4. Appendix

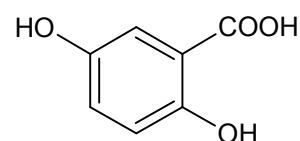
### 4.1. Chemical structure of ILM compounds



$\alpha$ -cyano-4-hydroxycinnamic  
acid (CHCA)

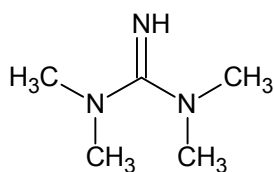


2,4,6-trihydroxyaceto-  
phenone (THAP)

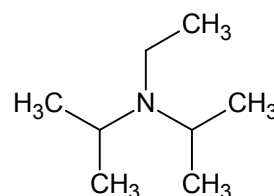


2,5-dihydroxybenzoic  
acid (DHB)

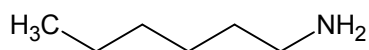
**Figure 4.1:** Chemical structure of acidic matrix compounds



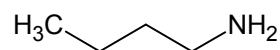
N,N,N',N'-tetramethylguanidinium  
(TGM)



N,N-diisopropylethylamine  
(DIEA)



hexylamine  
(HxA)



butylamine  
(BuA)

**Figure 4.2:** Chemical structure of basic matrix compounds



## 4.2. Ionic liquids used as matrices for MALDI-MS

**Table 4.1:** ILs used as matrices for MALDI-MS, references of their first use for MALDI-MS and the group of analytes investigated thereby. Seven of these ILs were tested the first time as ILMs.

Ionic liquid	Abbreviation	Previously reported	Analytes
<i>N,N,N',N'</i> -tetramethylguanidinium $\alpha$ -cyano-4-hydroxycinnamate	TMG-CHCA		
butylammonium $\alpha$ -cyano-4-hydroxycinnamate	BuA-CHCA	[7]	peptides, proteins, PEG
hexylammonium $\alpha$ -cyano-4-hydroxycinnamate	HxA-CHCA		
<i>N,N</i> -diisopropylethylammonium $\alpha$ -cyano-4-hydroxycinnamate	DIEA-CHCA	[25]	peptides, proteins, carbohydrates
<i>N,N,N',N'</i> -tetramethylguanidinium 2,4,6-trihydroxyacetophenone	TGM-THAP	[37]	peptides, glycans, glycopeptides
butylammonium 2,4,6-trihydroxyacetophenone	BuA-THAP		
hexylammonium 2,4,6-trihydroxyacetophenone	HxA-THAP		
<i>N,N</i> -diisopropylethylammonium 2,4,6-trihydroxyacetophenone	DIEA-THAP		
<i>N,N,N',N'</i> -tetramethylguanidinium 2,5-dihydroxybenzoate	TGM-DHB		
butylammonium 2,5-dihydroxybenzoate	BuA-DHB	[31]	proteins, peptides, glycans, ganglioside, oligosaccharides, PEG
hexylammonium 2,5-dihydroxybenzoate	HxA-DHB		
<i>N,N</i> -diisopropylethylammonium 2,5-dihydroxybenzoate	DIEA-DHB	[25]	peptides, proteins, carbohydrates

### 4.3. Bovine $\alpha$ 1-acid-glycoprotein

#### 4.3.1. The structure of bovine AGP

Bovine AGP consists of 202 amino acids including the signal peptide of 18 amino acids (not being present in the used sample). It contains one disulfide bond (between the amino acids 91 and 184) and five *N*-glycosylation sites. No other post-translational modifications are present. The primary structure of bovine AGP with its glycosylation and tryptic cleavage sites is given in Fig. 4.3.

1	<i>MALLWALAVL</i>	SHLPLLD <u>Q</u> S	<u>PECANLMTVA</u>	30
31	<u>PITNATMDLL</u>	<u>SGKWFYIGSA</u>	<u>FRNPEYNKSA</u>	60
61	<u>RAIQAAFFYL</u>	<u>EPRHAEDKLI</u>	<u>TREYQTIEDK</u>	90
91	<u>CVYNCSFIK</u> I	<u>YRQNGTLSKV</u>	<u>ESDREHFVDL</u>	120
121	<u>LLSKHFRTFM</u>	<u>LAASWNGTKN</u>	<u>VGVSFYADKP</u>	150
151	<u>EVTQEQQKEF</u>	<u>LDVIKCIGIQ</u>	<u>ESEIYTDEK</u>	180
181	<u>KDACGPLEKQ</u>	<u>HEEERKKETE</u>	<u>AS</u>	202

**Figure 4.3:** Primary structure of bovine AGP: Glycosylation sites are marked in dark blue letters. Tryptic peptides are specified alternately in orange and green letters, glycopeptides in blue letters. Glycosylation sites are marked in dark blue letters. The signal peptide is indicated in italic.

#### 4.3.2. Glycosylation of bovine AGP

Bovine AGP contains five *N*-glycosylation sites with bi- and triantennary complex type glycans [71]. The majority of the carbohydrate chains belongs to the biantennary type substituted with two to four terminal sialic acids (*N*-acetyl- and/or *N*-glycolyl-neuraminic acids). The triantennary glycan structures are carrying four or five sialic acids.

## **5. Literature**

1. Apweiler R, Hermjakob H, Sharon N. On the frequency of protein glycosylation, as deduced from analysis of the SWISS-PROT database. *Biochimica et Biophysica Acta* **1999**; 1473: 4-8.
2. Moens S, Vanderleyden J. Glycoproteins in prokaryotes. *Archives of Microbiology* **1997**; 168: 169-175.
3. Morelle W, Canis K, Chirat F, Faid V, Michalski J-C. The use of mass spectrometry for the proteomic analysis of glycosylation. *Proteomics* **2006**; 6: 3993-4015.
4. Sekiya S, Wada Y, Tanaka K. Derivatization for Stabilizing Sialic Acids in MALDI-MS. *Analytical Chemistry* **2005**; 77: 4962-4968.
5. Kang P, Mechref Y, Klouckova I, Novotny MV. Solid-phase permethylation of glycans for mass spectrometric analysis. *Rapid Communications in Mass Spectrometry* **2005**; 19: 3421-3428.
6. Papac DI, Wong A, Jones AJ. Analysis of acidic oligosaccharides and glycopeptides by matrix-assisted laser desorption/ionization time-of-flight mass spectrometry. *Analytical chemistry* **1996**; 68: 3215-23.
7. Armstrong DW, Zhang L-K, He L, Gross ML. Ionic liquids as matrixes for matrix-assisted laser desorption/ionization mass spectrometry. *Analytical Chemistry* **2001**; 73: 3679-3686.
8. Dzyuba SV, Bartsch RA. Expanding the polarity range of ionic liquids. *Tetrahedron Letters* **2002**; 43: 4657-4659.
9. Soukup-Hein RJ, Warnke MM, Armstrong DW. Ionic liquids in analytical chemistry. *Annual Review of Analytical Chemistry* **2009**; 2: 145-168.

10. Tsuda T, Hussey CL. Electrochemical applications of room-temperature ionic liquids. *Electrochemical Society Interface* **2007**; 16: 42-49.
11. Wei D, Ivaska A. Applications of ionic liquids in electrochemical sensors. *Analytica Chimica Acta* **2008**; 607: 126-135.
12. Han X, Armstrong DW. Ionic liquids in separations. *Accounts of Chemical Research* **2007**; 40: 1079-1086.
13. Shamsi SA, Danielson ND. Utility of ionic liquids in analytical separations. *Journal of Separation Science* **2007**; 30: 1729-1750.
14. Anderson JL, Armstrong DW. High-stability ionic liquids. A new class of stationary phases for gas chromatography. *Analytical Chemistry* **2003**; 75: 4851-4858.
15. Armstrong DW, He L, Liu Y-S. Examination of Ionic Liquids and Their Interaction with Molecules, When Used as Stationary Phases in Gas Chromatography. *Analytical Chemistry* **1999**; 71: 3873-3876.
16. Sun Y, Stalcup Apryll M. Mobile phase effects on retention on a new butylimidazolium-based high-performance liquid chromatographic stationary phase. *Journal of chromatography* **2006**; 1126: 276-82.
17. Polyakova Y, Koo YM, Row KH. Application of ionic liquids as mobile phase modifier in HPLC. *Biotechnology and Bioprocess Engineering* **2006**; 11: 1-6.
18. Stalcup AM, Cabovska B. Ionic liquids in chromatography and capillary electrophoresis. *Journal of Liquid Chromatography & Related Technologies* **2004**; 27: 1443-1459.
19. Qin W, Wei H, Li SFY. 1,3-Dialkylimidazolium-based room-temperature ionic liquids as background electrolyte and coating material in aqueous capillary electrophoresis. *Journal of Chromatography* **2003**; 985: 447-454.

20. Berthod A, He L, Armstrong DW. Ionic liquids as stationary phase solvents for methylated cyclodextrins in gas chromatography. *Chromatographia* **2001**; 53: 63-68.
21. Yanes EG, Gratz SR, Baldwin MJ, Robison SE, Stalcup AM. Capillary electrophoretic application of 1-Alkyl-3-methylimidazolium-based ionic liquids. *Analytical Chemistry* **2001**; 73: 3838-3844.
22. Huddleston JG, Rogers RD. Room temperature ionic liquids as novel media for 'clean' liquid-liquid extraction. *Chemical Communications* **1998**; 1765-1766.
23. Calvano CD, Carulli S, Palmisano F. Aniline/ $\alpha$ -cyano-4-hydroxycinnamic acid is a highly versatile ionic liquid for matrix-assisted laser desorption/ionization mass spectrometry. *Rapid Communications in Mass Spectrometry* **2009**; 23: 1659-1668.
24. Carda-Broch S, Berthod A, Armstrong DW. Ionic matrices for matrix-assisted laser desorption/ionization time-of-flight detection of DNA oligomers. *Rapid Communications in Mass Spectrometry* **2003**; 17: 553-560.
25. Crank Jeffrey A, Armstrong Daniel W. Towards a second generation of ionic liquid matrices (ILMs) for MALDI-MS of peptides, proteins, and carbohydrates. *J Am Soc Mass Spectrom* **2009**; 20: 1790-800.
26. Fukuyama Y, Nakaya S, Yamazaki Y, Tanaka K. Ionic Liquid Matrixes Optimized for MALDI-MS of Sulfated/Sialylated/Neutral Oligosaccharides and Glycopeptides. *Analytical Chemistry* **2008**; 80: 2171-2179.
27. Laremore TN, Linhardt RJ. Improved matrix-assisted laser desorption/ionization mass spectrometric detection of glycosaminoglycan disaccharides as cesium salts. *Rapid Communications in Mass Spectrometry* **2007**; 21: 1315-1320.
28. Laremore TN, Zhang F, Linhardt RJ. Ionic liquid matrix for direct UV-MALDI-TOF-MS analysis of dermatan sulfate and chondroitin sulfate oligosaccharides. *Analytical Chemistry* **2007**; 79: 1604-1610.

29. Li YL, Gross ML. Ionic-liquid matrices for quantitative analysis by MALDI-TOF mass spectrometry. *Journal of the American Society for Mass Spectrometry* **2004**; 15: 1833-1837.
30. Li YL, Gross ML, Hsu F-F. Ionic-liquid matrices for improved analysis of phospholipids by MALDI-TOF mass spectrometry. *Journal of the American Society for Mass Spectrometry* **2005**; 16: 679-682.
31. Mank M, Stahl B, Boehm G. 2,5-Dihydroxybenzoic acid butylamine and other ionic liquid matrixes for enhanced MALDI-MS analysis of biomolecules. *Analytical Chemistry* **2004**; 76: 2938-2950.
32. Naumann I, Darsow KH, Walter C, Lange HA, Buchholz R. Identification of sulfoglycolipids from the alga *Porphyridium purpureum* by matrix-assisted laser desorption/ionisation quadrupole ion trap time-of-flight mass spectrometry. *Rapid Communications in Mass Spectrometry* **2007**; 21: 3185-3192.
33. Schnoell-Bitai I, Ullmer R, Hrebicek T, Rizzi A, Lacik I. Characterization of the molecular mass distribution of pullulans by matrix-assisted laser desorption/ionization time-of-flight mass spectrometry using 2,5-dihydroxybenzoic acid butylamine (DHBB) as liquid matrix. *Rapid Communications in Mass Spectrometry* **2008**; 22: 2961-2970.
34. Tholey A. Ionic liquid matrices with phosphoric acid as matrix additive for the facilitated analysis of phosphopeptides by matrix-assisted laser desorption/ionization mass spectrometry. *Rapid Communications in Mass Spectrometry* **2006**; 20: 1761-1768.
35. Tissot B, Gasiunas N, Powell AK, Ahmed Y, Zhi Z-I, Haslam SM, Morris HR, Turnbull JE, Gallagher JT, Dell A. Towards GAG glycomics: Analysis of highly sulfated heparins by MALDI-TOF mass spectrometry. *Glycobiology* **2007**; 17: 972-982.

36. Towers Mark W, McKendrick John E, Cramer R. Introduction of 4-chloro-alpha-cyanocinnamic acid liquid matrices for high sensitivity UV-MALDI MS. *Journal of proteome research* **2010**; 9: 1931-40.
37. Ullmer R, Rizzi AM. Use of a novel ionic liquid matrix for MALDI-MS analysis of glycopeptides and glycans out of total tryptic digests. *Rapid Communications in Mass Spectrometry* **2009**; 44: 1596-1603.
38. Zabet-Moghaddam M, Heinzle E, Lasaosa M, Tholey A. Pyridinium-based ionic liquid matrices can improve the identification of proteins by peptide mass-fingerprint analysis with matrix-assisted laser desorption/ionization mass spectrometry. *Analytical and Bioanalytical Chemistry* **2006**; 384: 215-224.
39. Zabet-Moghaddam M, Krueger R, Heinzle E, Tholey A. Matrix-assisted laser desorption/ionization mass spectrometry for the characterization of ionic liquids and the analysis of amino acids, peptides and proteins in ionic liquids. *Journal of Mass Spectrometry* **2004**; 39: 1494-1505.
40. Arenz S, Babai A, Binnemans K, Driesen K, Giernoth R, Mudring A-V, Nockemann P. Intense near-infrared luminescence of anhydrous lanthanide(III) iodides in an imidazolium ionic liquid. *Chemical Physics Letters* **2005**; 402: 75-79.
41. Berthod A, Crank JA, Rundlett KL, Armstrong DW. A second-generation ionic liquid matrix-assisted laser desorption/ionization matrix for effective mass spectrometric analysis of biodegradable polymers. *Rapid Communications in Mass Spectrometry* **2009**; 23: 3409-3422.
42. Soukup-Hein RJ, Remsburg JW, Dasgupta PK, Armstrong DW. A General, Positive Ion Mode ESI-MS Approach for the Analysis of Singly Charged Inorganic and Organic Anions Using a Dicationic Reagent. *Analytical Chemistry* **2007**; 79: 7346-7352.
43. Remsburg JW, Soukup-Hein RJ, Crank JA, Breitbach ZS, Payagala T, Armstrong DW. Evaluation of dicationic reagents for their use in detection of

- anions using positive ion mode ESI-MS via gas phase ion association. *Journal of the American Society for Mass Spectrometry* **2008**; 19: 261-269.
44. Soukup-Hein RJ, Remsburg JW, Breitbach ZS, Sharma PS, Payagala T, Wanigasekara E, Huang J, Armstrong DW. Evaluating the Use of Tricationic Reagents for the Detection of Doubly Charged Anions in the Positive Mode by ESI-MS. *Analytical Chemistry* **2008**; 80: 2612-2616.
  45. Billard I, Mekki S, Gaillard C, Hesemann P, Moutiers G, Mariet C, Labet A, Buenzli J-CG. EuIII luminescence in a hygroscopic ionic liquid: effect of water and evidence for a complexation process. *European Journal of Inorganic Chemistry* **2004**; 1190-1197.
  46. Driesen K, Nockemann P, Binnemans K. Ionic liquids as solvents for near-infrared emitting lanthanide complexes. *Chemical Physics Letters* **2004**; 395: 306-310.
  47. Alvaro M, Ferrer B, Fornes V, Garcia H, Scaiano JC. Bipyridinium macro-ring encapsulated within zeolite Y supercages. Preparation and intrazeolitic photochemistry of a common electron acceptor component of rotaxanes and catenanes. *Journal of Physical Chemistry* **2002**; 106: 6815-6820.
  48. Crowhurst L, Lancaster NL, Perez Arlandis JM, Welton T. Manipulating Solute Nucleophilicity with Room Temperature Ionic Liquids. *Journal of the American Chemical Society* **2004**; 126: 11549-11555.
  49. Wasserscheid P, Boesmann A, Bolm C. Synthesis and properties of ionic liquids derived from the "chiral pool". *Chemical Communications* **2002**; 200-201.
  50. Koel M. Ionic Liquids in Chemical Analysis. *Critical Reviews in Analytical Chemistry* **2005**; 35: 177-192.
  51. Berthod A, Carda-Broch S. Uses of ionic liquids in chemical analysis. *Actualite Chimique* **2004**; 24-30.



52. Baker GA, Baker SN, Pandey S, Bright FV. An analytical view of ionic liquids. *Analyst* **2005**; 130: 800-808.
53. Karas M, Hillenkamp F. Laser desorption ionization of proteins with molecular masses exceeding 10,000 daltons. *Analytical chemistry* **1988**; 60: 2299-301.
54. Cohen LH, Gusev AI. Small molecule analysis by MALDI mass spectrometry. *Analytical and Bioanalytical Chemistry* **2002**; 373: 571-586.
55. Stoeckli M, Farmer TB, Caprioli RM. Automated mass spectrometry imaging with a matrix-assisted laser desorption ionization time-of-flight instrument. *Journal of the American Society for Mass Spectrometry* **1999**; 10: 67-71.
56. Aebersold R, Mann M. Mass spectrometry-based proteomics. *Nature* **2003**; 422: 198-207.
57. Laremore TN. MALDI-MS applications in glycomics of glycosaminoglycans. *Rensselaer Polytechnic Institute, Troy, NY, USA* **2007**; 91 pp.
58. Garden RW, Sweedler JV. Heterogeneity within MALDI samples as revealed by mass spectrometric imaging. *Analytical chemistry* **2000**; 72: 30-6.
59. Nicola AJ, Gusev AI, Proctor A, Jackson EK, Hercules DM. Application of the fast-evaporation sample preparation method for improving quantification of angiotensin II by matrix-assisted laser desorption/ionization. *Rapid Communications in Mass Spectrometry* **1995**; 9: 1164-71.
60. Distler AM, Allison J. Improved MALDI-MS analysis of oligonucleotides through the use of fucose as a matrix additive. *Analytical Chemistry* **2001**; 73: 5000-5003.
61. Lemaire R, Tabet JC, Ducoroy P, Hendra JB, Salzet M, Fournier I. Solid Ionic Matrixes for Direct Tissue Analysis and MALDI Imaging. *Analytical Chemistry* **2006**; 78: 809-819.

62. Zabet-Moghaddam M, Heinzle E, Tholey A. Qualitative and quantitative analysis of low molecular weight compounds by ultraviolet matrix-assisted laser desorption/ionization mass spectrometry using ionic liquid matrices. *Rapid Communications in Mass Spectrometry* **2004**; 18: 141-148.
63. Cramer R, Corless S. Liquid ultraviolet matrix-assisted laser desorption/ionization - mass spectrometry for automated proteomic analysis. *Proteomics* **2005**; 5: 360-370.
64. Darsow Kai H, Lange Harald A, Resch M, Walter C, Buchholz R. Analysis of a chlorosulfolipid from *Ochromonas danica* by matrix-assisted laser desorption/ionization quadrupole ion trap time-of-flight mass spectrometry. *Rapid Communications in Mass Spectrometry* **2007**; 21: 2188-94.
65. Laremore TN, Murugesan S, Park T-J, Avci FY, Zagorevski DV, Linhardt RJ. Matrix-Assisted Laser Desorption/Ionization Mass Spectrometric Analysis of Uncomplexed Highly Sulfated Oligosaccharides Using Ionic Liquid Matrices. *Analytical Chemistry* **2006**; 78: 1774-1779.
66. Jones JJ, Batoy SMAB, Wilkins CL, Liyanage R, Lay JO. Ionic Liquid Matrix-Induced Metastable Decay of Peptides and Oligonucleotides and Stabilization of Phospholipids in MALDI FTMS Analyses. *Journal of the American Society for Mass Spectrometry* **2005**; 16: 2000-2008.
67. Chan K, Lanthier P, Liu X, Sandhu JK, Stanimirovic D, Li J. MALDI mass spectrometry imaging of gangliosides in mouse brain using ionic liquid matrix. *Analytica Chimica Acta* **2009**; 639: 57-61.
68. Domon B, Costello CE. A systematic nomenclature for carbohydrate fragmentations in FAB-MS/MS spectra of glycoconjugates. *Glycoconjugate Journal* **1988**; 5: 397-409.
69. Harvey DJ. Fragmentation of Negative Ions from Carbohydrates: Part 2. Fragmentation of High-Mannose N-Linked Glycans. *Journal of the American Society for Mass Spectrometry* **2005**; 16: 631-646.

70. Harvey DJ. Fragmentation of Negative Ions from Carbohydrates: Part 3. Fragmentation of Hybrid and Complex N-Linked Glycans. *Journal of the American Society for Mass Spectrometry* **2005**; 16: 647-659.
71. Nakano M, Kakehi K, Tsai M-H, Lee YC. Detailed structural features of glycan chains derived from alpha 1-acid glycoproteins of several different animals: the presence of hypersialylated, O-acetylated sialic acids but not disialyl residues. *Glycobiology* **2004**; 14: 431-441.

## **6. Abstract**

In detail characterization of oligosaccharide structures attached to proteins is an essential step in developing substantial understanding in which subtle varieties glycosylation can occur and how it influences biological properties of proteins. Matrix-assisted laser desorption/ionization mass spectrometry (MALDI-MS) of glycopeptides gained from glycoproteins by enzymatic digestion is an established tool for glycosylation research. For this method, the detection of minor abundant and small glycopeptides and glycans out of the proteolytic digest containing a large amount of non-glycosylated peptides is often impeded by ionization suppression effects. Furthermore, the analysis of sialylated oligosaccharides is limited by the labile nature of sialic acid residues.

There are several approaches to overcome these problems, the most commonly used is the pre-separation of the glycopeptides/glycans prior to MS analysis. As an alternative approach the development and use of ionic liquid matrices (ILMs) as alternative MALDI matrices for glycopeptide/glycan analysis is investigated in this work. Twelve different ionic liquids were synthesized by combination of conventional MALDI matrices with four different organic bases and applied as ILMs. The tryptic digest of bovine  $\alpha$ 1-acid-glycoprotein (representing a typical mixture of glycosylated and non-glycosylated peptides), and the same digest after treatment with an endoglycosidase (representing a typical mixture of released neat glycans and peptides) were used as test samples. Among the ILMs tested, butylammonium 2,4,6-trihydroxyacetophenone (BuA-THAP), *N,N,N',N'*-tetramethylguanidinium 2,4,6-trihydroxyacetophenone (TGM-THAP) and *N,N*-diisopropylethylammonium  $\alpha$ -cyano-4-hydroxycinnamate (DIEA-CHCA), all in combination with di-ammonium hydrogen phosphate as matrix solution additive, were found to be best in overcoming the ionization suppression effects with glycans and glycopeptides in the presence of non-glycosylated peptides. This result was observed in the positive as well as in the negative ionization mode and allowed to attain an increased sequence coverage compared to the use of the common solid matrices  $\alpha$ -cyano-4-hydroxycinnamic acid and 2,4,6-trihydroxyacetophenone (THAP).

Importantly, glycopeptides and neat glycans were detected with signal intensities sufficient for MS/MS analysis which is an essential requirement for structural analysis. The loss of terminal labile sialic acid groups was reduced when using ILMs, but not completely avoided. Particularly in the negative ionization mode intact glycans with all sialic acids attached could be detected.

The limits of detection (LODs) of glycopeptides in the peptide mixture were worse when comparing to THAP, but strongly improved in the case of cleaved glycans. The expected increase in reproducibility of signal intensities, which should be expected because of the liquid consistency of the ILMs, could not be observed. “Hot spot” selection was not longer necessary, leading to decreased measurement times. In summary, the use of ILMs for the particular purpose of glycosylation analysis of proteins was found being appropriate and useful as an alternative to the use of conventional crystalline matrices.

## **7. Zusammenfassung**

Die detaillierte Charakterisierung der Glykosylierung von Proteinen ist essentiell für die Entwicklung eines umfangreichen Verständnisses dafür, in welcher Vielfalt Oligosaccharidstrukturen vorkommen und wie diese die biologischen Eigenschaften von Proteinen beeinflussen. Die Matrix-unterstützte Laser Desorption/Ionisation-Massenspektrometrie (MALDI-MS) ist eine etablierte Methode zur Untersuchung der Glykosylierungen von Glykopeptiden. Bei MALDI wird die Ionisationsausbeute von Glykanen und kleinen Glykopeptiden in einer Mischung mit nicht-glykosylierten Peptiden gewöhnlich durch Ionisationsunterdrückungseffekte beeinträchtigt. Dies ist beispielsweise bei proteolytischen Verdauen von Glykoproteinen der Fall. Darüber hinaus ist die MALDI-Analyse von sialinsäurehaltigen Oligosaccharidstrukturen durch den labilen Bindungscharakter der Sialinsäurereste eingeschränkt.

Es gibt mehrere Ansätze, um die Probleme der Ionisierungsunterdrückung zu überwinden; der am häufigsten verwendete ist die Trennung der Glykopeptide/Glykane von nicht-glykosylierten Peptiden vor der MS-Analyse. Als ein alternativer Ansatz wird in dieser Arbeit die Entwicklung und Verwendung von ionisch-flüssigen Matrices (ILMs) für die Glykopeptid/Glykan-Analyse in Gegenwart von nicht-glykosylierten Peptiden untersucht. Durch die Kombination von drei konventionellen MALDI-Matrices mit vier verschiedenen organischen Basen wurden zwölf verschiedene ionische Flüssigkeiten synthetisiert und als ILMs angewandt. Als Test-Proben wurden der tryptische Verdau von aus Rinderblutplasma gewonnenem  $\alpha$ 1-sauren Glykoprotein (entspricht einer typischen Mischung von glykosylierten und nicht-glykosylierten Peptiden) und der gleiche Verdau nach der Behandlung mit einer Endoglykosidase (entspricht einer typischen Mischung von Peptiden und abgespaltenen Glykanen) gewählt. Unter den getesteten ILMs waren Butylammonium-2,4,6-trihydroxyacetophenon (BuA-THAP), *N,N,N',N'*-Tetramethylguanidinium-2,4,6-trihydroxyacetophenon (TGM-THAP) und *N,N*- $\alpha$ -Diisopropylethylammonium-cyano-4-hydroxycinnamat (DIEA-CHCA) - alle in Kombination mit Diammoniumhydrogenphosphat als Matrix-Lösungszusatz - am besten geeignet, die Ionisierungsunterdrückung von Glykanen und Glykopeptiden in Gegenwart von nicht-glykosylierten Peptiden zu minimieren. Dieses Ergebnis wurde im positiven wie im

negativen Ionisationsmodus erzielt und ermöglichte eine erhöhte Peptidsequenzabdeckung im Vergleich zu herkömmlichen kristallinen Matrices (2,4,6-Trihydroxyacetophenon (THAP) und  $\alpha$ -Cyano-4-hydroxysäure).

Die Glykopeptide wie auch die Glykane konnten mit ausreichend hohen Signalintensitäten für MS/MS-Messungen detektiert werden. Dies ist eine wesentliche Voraussetzung für strukturelle Analysen. Die Abspaltung der labilen terminalen Sialinsäuren konnte durch die Anwendung der ILMs zwar reduziert, aber nicht vollständig verhindert werden. Besonders im negativen Ionisierungsmodus konnten intakte Glykane, an die noch alle Sialinsäuren gebunden waren, nachgewiesen werden.

Die Nachweisgrenzen (LODs) für Glykopeptide in einem Peptid-Gemisch hatten sich im Vergleich zu THAP verschlechtert, für Glykane jedoch stark verbessert. Eine erhöhte Reproduzierbarkeit von Signalintensitäten, die aufgrund der flüssigen Konsistenz der ILMs erwartet werden konnte, wurde nicht beobachtet. Die Suche nach sogenannten "Hot Spots" war nicht mehr notwendig. Dadurch konnten verkürzte Messzeiten erreicht werden.

Zusammenfassend war die Anwendung von ILMs für die MALDI-MS-Analyse von Proteinglykosylierungen geeignet und stellt eine nützliche Alternative zur Anwendung von herkömmlichen kristallinen Matrices dar.





# **CURRICULUM VITAE**

## **PERSÖNLICHE DATEN**

---

Name:	Manuela Kropik
Geburtsdatum:	30.09.1975
Geburtsort:	Linz
Staatbürgerschaft:	Österreich
Familienstand:	ledig

## **AUSBILDUNG**

---

12/2009-09/2010	Diplomarbeit am Institut für Analytische Chemie, Arbeitsgruppe Univ.-Prof. Dr. Andreas Rizzi
03/1999	Umstieg auf Diplomstudium Chemie
10/1995	Beginn des Diplomstudiums Biochemie an der Universität Wien
1991-1995	Oberstufenrealgymnasium der Diözese Linz, naturwissenschaftlicher Zweig
1986-1991	Akademisches Gymnasium, Linz

## **BERUFLICHE TÄTIGKEITEN**

---

09/2004-11/2009	H&M Hennes & Mauritz Gesmbh (Angestellte)
04/2004-09/2004	sale4U Vertriebsgmbh (freier DV)
02/1997-12/2003	Telekom Austria (geringfügig besch. / freier DV)
07/2000-08/2000	Land Oberösterreich (Angestellte)
08/1999-09/1999	Land Oberösterreich (Angestellte)